

AN ANALYSIS OF LAMINAR JET REATTACHMENT:
REATTACHMENT DISTANCE AS A FUNCTION OF REYNOLDS NUMBER

by
Felix Aguilar

Thesis submitted to the Graduate Faculty of the
Virginia Polytechnic Institute
in candidacy for the degree of
Master of Science
in
Mechanical Engineering

Approved:

Dr. R. A. Comparin, Chairman

Dr. F. J. Pierce

Dr. J. B. Jones, Head of Department

November, 1968
Blacksburg, Virginia

TABLE OF CONTENTS

Chapter	Page
LIST OF FIGURES & TABLES.....	iv
NOMENCLATURE.....	v
I. INTRODUCTION.....	1
II. REVIEW OF LITERATURE.....	5
Two-Dimensional Laminar Jet Flow.....	5
Jet Reattachment to an Adjacent Flat Plate.....	6
III. ANALYSIS.....	9
General Solution.....	9
Two-Dimensional Laminar Jet Theory.....	16
1. The Bickley Solution.....	16
2. The Okabe Approximate Solution.....	18
3. The Modified Okabe Solution.....	21
Reattachment Distance versus Reynolds Number.....	27
1. The Analysis with the Bickley Profile.....	27
2. The Analysis with the Okabe Profile.....	30
3. The Analysis with the Modified Okabe Profile..	34
IV. RESULTS.....	37
V. ACKNOWLEDGEMENTS.....	46
VI. BIBLIOGRAPHY.....	47
VII. VITA.....	49
VIII. APPENDICES.....	50
A. Integration of the Square of the Velocity Functions of the Okabe and Modified Okabe Solutions.....	50

	Page
B. Application of the Gaussian Quadrature	
Method.....	56
C. Computer Programs.....	61
Determination of Reattachment Distance versus Reynolds Number Using the Bickley Exact Solution for the Laminar Plane Jet...	62
Determination of Reattachment Distance versus Reynolds Number Using the Okabe Approximate Solution for the Laminar Plane Jet.....	66
Determination of Reattachment Distance versus Reynolds Number Using the Modified Okabe Approximate Solution for the Laminar Plane Jet.....	76
D. Comments on Thomas' Modification of the Okabe Solution.....	86

LISTS OF FIGURES & TABLES

Figure	Page
1. The control volume approach to the problem of jet reattachment at low Reynolds numbers.....	3
2. Jet reattachment to an inclined flat plate.....	11
3. Velocity distributions of the laminar plane jet: Bickley, Okabe, modified Okabe.....	26
4. Laminar jet reattachment to a flat plate inclined at 25°.....	40
5. Laminar jet reattachment to a flat plate inclined at 30°.....	41
6. Laminar jet reattachment to a flat plate inclined at 40°.....	42
7. Laminar jet reattachment to a flat plate inclined at 50°.....	43
Table	
1. Approximate solutions for the plane jet.....	22
2. The proportionality constant C_1 for various plate inclinations.....	39

NOMENCLATURE

Symbols

a	scale factor found in equation 3
b	width of nozzle exit
C_1	dimensionless constant
C_2	dimensionless constant
C_p	pressure coefficient: $C_p = (P_B - P_\infty)/(P_0 - P_\infty)$
J	momentum flux
P	static pressure
P_0	stagnation pressure of fluid supplying jet
P_∞	static pressure of surroundings
P_B	static pressure within separation bubble
Re	Reynolds number: $Re = U b/\nu$
r	magnitude of path vector defined by equation 3
s	arc distance measured along reattaching streamline
u	x-component of velocity
U	mean velocity of mass leaving nozzle
(x,y)	Cartesian coordinates: x coincident with axis of a free two-dimensional jet
x'	coordinate measured from virtual origin of a two-dimensional jet
X_r	reattachment distance measured along inclined plate from nozzle exit to point of reattachment
α	angle of plate inclination

β	angle between reattaching streamline and path vector
γ	angle between reattaching streamline and plate at reattachment
ϕ	angle between path vector and initial direction of jet
ϕ_m	maximum possible value of ϕ
δ	dimensionless jet width: $\delta = 2\Delta/b$
Δ	distance from axis of symmetry to boundary of jet
η	dimensionless ordinate: $\eta = y/\Delta$
θ	dimensionless velocity component: $\theta = u/U$
ρ	density
λ	parameter dependent on x
ν	kinematic viscosity
ξ	dimensionless ordinate defined by equation 10b

Subscripts

r	quantity referred to the reattachment point
-----	---

I. INTRODUCTION

The problem of jet reattachment to an adjacent plate is of great concern to fluidics technology. An analytical formulation of the reattachment phenomenon describing both the flow field and the pressure field is immediately applicable to fluidic design. In the solution of the problem lie the solutions to other problems such as those dealing with the effect of the injection of mass through a control jet and with the calculation of the corresponding response time.

However, most of the present literature on jet reattachment considers only high Reynolds number turbulent jets. When this kind of jet attaches itself to an adjacent wall, the location of the reattachment point is independent of Reynolds number. By the choice of an appropriate jet spread parameter and by the stipulation of proper velocity conditions at the jet orifice, reattachment distance has been found to be only a function of plate angle and offset distance.

It is quite interesting to discover that the behavior of a stable laminar jet (low Reynolds number) is markedly different. Besides the dependence on plate angle and offset distance, the location of reattachment is strongly dependent on both Reynolds number and aspect ratio. Investigators in the area also hold suspect the initial development of the jet as a contributor to the reattachment phenomenon.

Unlike efforts made in the high Reynolds number range, analysis of laminar jet reattachment has been only moderately successful. The approach used thus far has been that developed by Bourque and Newman for the high Reynolds number case (4). The boundaries of a semi-infinite control volume are drawn about the reattachment zone as shown in Figure 1. The principle of momentum conservation is then applied to the control volume. In conjunction with the consideration of the equation of continuity and of the pertinent geometry, one may readily solve for the reattachment distance,

$$\frac{X_r}{b} = C_1 Re - C_2.$$

A number of assumptions are implicit to the solution, and among them are the following. The velocity profile of the jet is uniform at the nozzle exit, and the subsequent jet growth is governed by the velocity distribution for a laminar jet cited by Schlichting (14). Also the path of the jet center line is assumed to be a circular arc.

The aim of the present study is to delete the above assumptions from the analysis. Altogether, three solutions are developed. In the first, the previous solution is modified only in that the increasing curvature of the jet center line is taken into account. A uniform velocity profile is still assumed in the second analysis, however the jet growth is described by Okabe's approximate solution (8). Also the increasing curvature of the jet center line is considered. In the third solution, the second analysis is

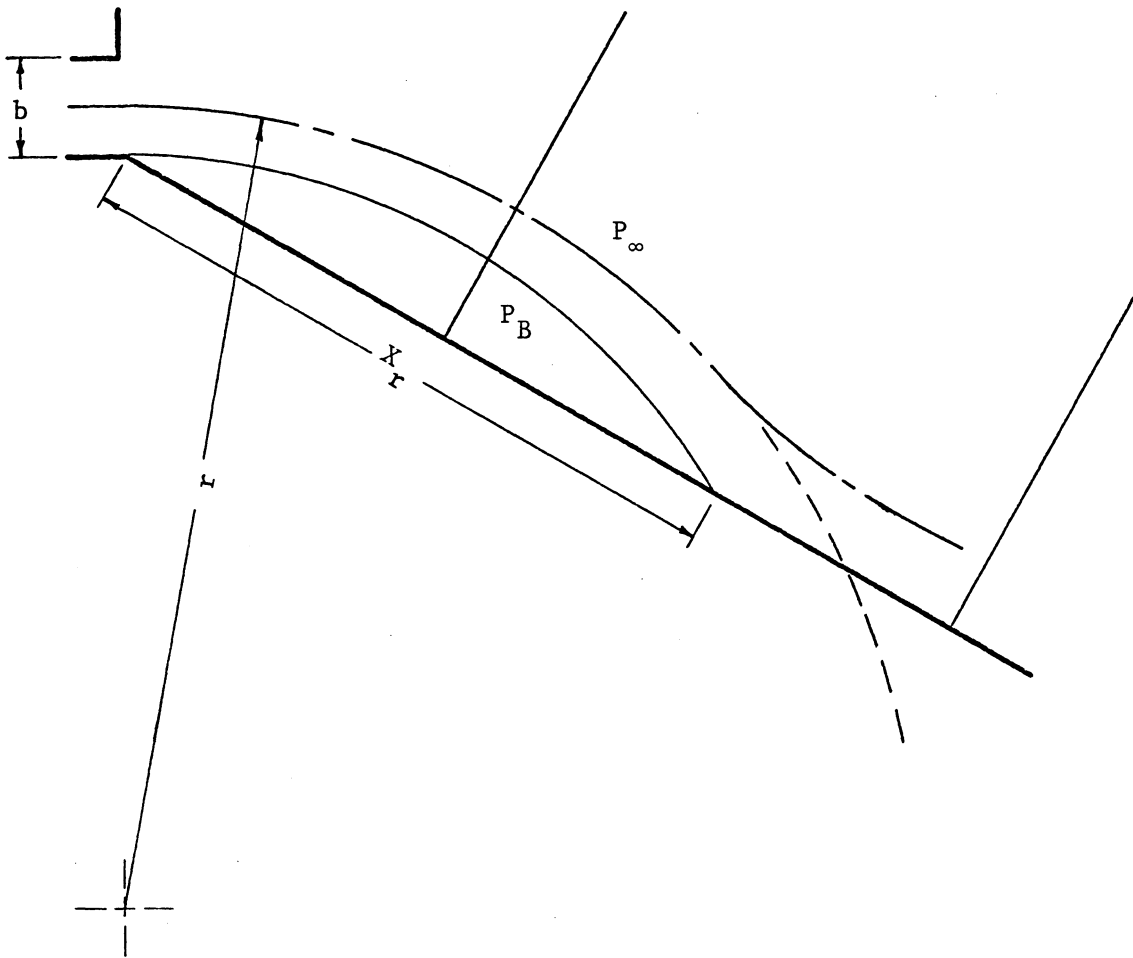


Figure 1. The control volume approach to the problem of jet reattachment at low Reynolds numbers

modified in an attempt to consider the effect of the emergence of a fully developed jet from the nozzle.

II. REVIEW OF LITERATURE

A very thorough survey of the literature related to jet reattachment necessarily would be a very ponderous document. The present state of the technology in this area is the fruit of progress in nearly every realm of fluid mechanics. Obviously the following survey has important omissions; but none is felt to be immediately pertinent to the task at hand.

Two-Dimensional Laminar Jet Flow

The initial work in the area of laminar jet flows was done in 1933 by H. Schlichting (13) who developed closed form expressions describing the behavior of the axially symmetrical laminar jet. A similar closed form solution for the case of the plane (two-dimensional) jet eluded Schlichting; and in 1937, W. G. Bickley (2) discovered that the equation for the plane case was indeed exactly integrable. This famous solution possessed a singularity at the jet origin (a characteristic of many exact solutions of the boundary layer equations) and was valid only at moderate to large distances from the origin. The solution was also encumbered by the necessity of determining a virtual origin if the solution were to be put to use. With some qualification, E. N. Andrade (1) confirmed the theory experimentally. Agreement between theory and fact was deemed to be best at low Reynolds numbers.

In 1948, J. Okabe (8) developed relatively complex but no less interesting solutions for both the plane and axially symmetrical

laminar jets. Okabe's approximate solutions dealt with jets emerging from orifices of finite dimension and having uniform velocity profiles. In addition, these solutions were applicable everywhere along the jet length. They satisfied the boundary layer equations exactly only at the extremities and centers of the jets. However with a numerical example, Okabe (9) showed that the net deviation was zero. A. L. Thomas (15) compared the Okabe velocity distribution for the plane laminar jet with Andrade's data and found the agreement to be quite good.

In the same paper, Thomas modified Okabe's approximate solution for the plane jet in an attempt to describe the behavior of a jet which emerged fully developed from a slit orifice. The effect of pressure gradient on momentum flux however was overly appraised, and in the opinion of this writer, this fact has seriously threatened Thomas's arguments. Criticism of Thomas's paper may be found in Appendix D.

Jet Reattachment to an Adjacent Flat Plate

Until very recently most effort in the area of jet reattachment has been expended in research concerning high Reynolds number turbulent plane jets attaching to adjacent flat plates. In 1960, C. Bourque and B. G. Newman (4) developed two approximate theories for the mean pressure within the separation bubble, for the position of reattachment, and for the increase in volume flow from the slot. Their interest was restricted to the range of

Reynolds numbers in which jet reattachment is independent of Reynolds number, and the investigation was qualified by the following assumptions: (i) the jet flow was incompressible and two-dimensional, (ii) the flow velocity was uniform at the exit from the slot, (iii) the pressure within the separation bubble was uniform and the center line of the jet was a circular arc, (iv) the jet had a velocity distribution of a free jet and entrained corresponding amounts of fluid, (v) entrainment within the bubble ceased and the flow divided where the extended center line of the jet intersected the plate, and (vi) the force parallel to the plate due to the skin friction of the forward and backward flow near reattachment was negligible compared with jet momentum. Bourque and Newman attacked the problem from two points of view. In their first theory the momentum principle was applied locally at the reattachment point neglecting the pressure difference across the extended jet center line. As depicted in Figure 1, a control volume extending from midway along the jet center line and past the reattachment point was considered in the second theory. Bourque and Newman found the agreement between analysis and experiment to be fairly satisfactory.

In the same year, R. A. Sawyer (11) experimentally supported the work of Bourque and Newman. Sawyer also suggested adjustment of the spread parameter (found in the Goertler velocity profile) as a convenient device for balancing error inherent in the analytic hypothesis. His measurements also induced him to

investigate the effect of curvature on jet entrainment. In 1963, Sawyer (12) modified the analysis to take into account the different rates of entrainment at the edges of the curved jet. He also made other refinements by including in the mathematical model a partially developed velocity profile at the jet orifice and the pressure forces near reattachment. Although the resulting calculations were quite complex, his efforts were vindicated experimentally.

By revising his previous hypothesis, Bourque (3) was able to make rather simple calculations which correlated quite well with his experimental data (reattachment distance versus plate angle). The revision postulated a sinusoidal variation of the vector radius of the path of the reattaching streamline. This simply presumed that the pressure difference across the jet increased up to the point of reattachment, implying that the curvature of the path increased as well. In qualitative terms this was accurate.

Jet reattachment at low Reynolds numbers had not been studied quantitatively until 1967 when R. A. Comparin, W. C. Jenkins, and R. B. Moore (5) published their measurements of jet reattachment distances on inclined walls with Reynolds numbers in the range 10 to 1400. It was found that reattachment distance varied approximately linearly with Reynolds number as long as a stable laminar jet was maintained. It was also observed that the location of this linear function was dependent on aspect ratio. Comparin's analysis, patterned after that of Bourque and Newman, yielded reasonable results only at high angles of wall inclination.

III. ANALYSIS

In the presentation of the various solutions for reattachment at low Reynolds numbers, the format is the following. First a general solution for reattachment distance is presented which--as cited in the introduction--incorporates the sinusoidal variation of the vector radius of the jet path. Then there follows a discussion of three solutions for the velocity field of a two-dimensional laminar jet: the Bickley, Okabe, and modified Okabe solutions. Finally, each velocity profile is substituted into the general solution in order to determine the functional dependence of reattachment distance on Reynolds number for each case. Experimental evidence is inserted in the text wherever justified, and computer programs and discussion of a few mathematical details appear in the appendices.

General Solution

The general solution is the same as the one developed by Bourque (3) for the case of turbulent jet reattachment to an adjacent flat plate. The following assumptions are necessary for the development of the theory:

- i) the jet aspect ratio is large, and the flow is everywhere two-dimensional, laminar, and incompressible.
- ii) the reattaching streamline effectively divides the flow.

- iii) at reattachment, momentum is conserved on both sides of the reattaching streamline even though the velocity profiles may be highly perturbed.
- iv) the jet width is small compared to the radius of curvature, and the distance measured along the reattaching streamline is equal to the distance measured along the jet center line.
- v) the velocity profile of the curved jet up to reattachment is that of a free jet, and the jet entrains corresponding amounts of fluid. The jet entrainment ceases where the reattaching streamline intersects the wall.
- vi) the pressure forces can be neglected in the momentum equation at reattachment.

The geometry of the flow is described in Figure 2.

The ordinate of the reattaching streamline can be determined from the equation of continuity. Since the flow is steady and reattachment is presumed stable, the mass flow between the jet center line and the reattaching streamline is equal to half the mass flow at the nozzle exit at every point along the jet,

$$\rho \frac{U_b}{2} = \int_0^{y_r} \rho u \, dy.$$

And since the flow is incompressible, the ordinate is given implicitly as

$$b = 2 \int_0^{y_r} \theta \, dy. \quad (1)$$

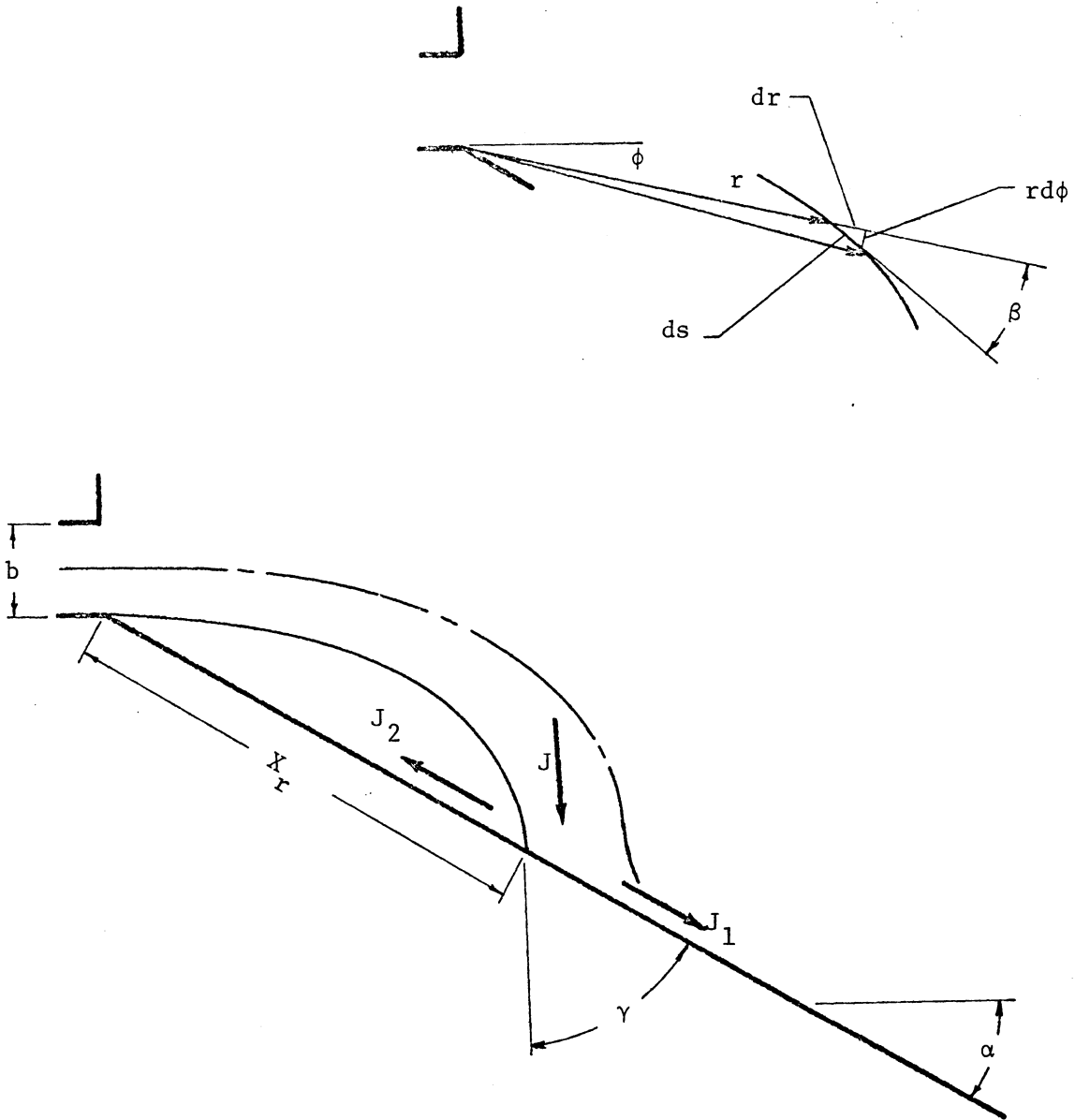


Figure 2. Jet reattachment to an inclined flat plate

With the geometry of Figure 2 in mind, Newton's second law may be written about the reattachment point,

$$\sum \overline{\text{forces}} = \frac{d}{dt} (\overline{\text{momentum}}).$$

In the direction coincident with the wall and with the application of assumptions ii, iii, and vi, the equation becomes

$$0 = (-J) \cos \gamma + J_1 - J_2.$$

And finally,

$$\cos \gamma = \frac{J_1 - J_2}{J}. \quad (2)$$

At this juncture, it is assumed that the pressure field corresponding to laminar jet reattachment is similar in nature to the pressure field for the high Reynolds number case. The pressure inside the separation bubble is not constant, and measurements performed by Bourque and Newman (4) reveal that the pressure coefficient C_p along the adjacent wall decreases with distance and then increases rapidly just before reattachment. The point of minimum pressure is closer to the reattachment point than to the nozzle exit. Thus Bourque (3) reports that the pressure difference across the jet increases during the first seven-tenths of the distance between the nozzle exit and the reattachment point and that it is impossible to determine the variation thereafter. With some justification therefore, he assumes that the pressure difference across the jet increases up to reattachment. In this

assumption lies the tacit assertion that the curvature of the path increases as the reattachment point is approached.

As will be seen in a following section, equations 1 and 2 predict that as reattachment distance is infinitely increased

$$\lim_{X_r \rightarrow \infty} \cos \gamma = 0.$$

This fact indicates that when the inclination of the plate is adjusted so that the reattachment point is an infinite distance from the nozzle exit, the resulting angle of reattachment will be 90 degrees. It is impossible to satisfy this condition by the previously postulated circular arc path. Moore (7) has measured this limiting angle of plate inclination to be 60 degrees for reattachment at low Reynolds numbers.

A function which satisfies the above condition and the condition of increasing curvature has been proposed by Rodrigue (3):

$$\frac{r}{b} = \frac{a}{b} \sin \left(\frac{\pi \phi}{2 \phi_m} \right). \quad (3)$$

The quantity a is a scale factor which is a function of the plate angle α , and its value increases from zero to infinity as α varies from zero to ϕ_m .

The following relations are evident from the geometry:

$$\alpha = \phi_r \quad \text{and} \quad \gamma = \beta_r.$$

Also from Figure 2, it may be seen that

$$\tan \beta = \frac{(r/b) d\phi}{d(r/b)}. \quad (4)$$

Differentiating equation 3 with respect to ϕ yields

$$\frac{d(r/b)}{d\phi} = \frac{\pi}{2\phi_m} \frac{a}{b} \cos \left(\frac{\pi}{2} \frac{\phi}{\phi_m} \right). \quad (5)$$

And finally after substitution of equations 3 and 5, equation 4 becomes

$$\tan \beta = \frac{2\phi_m}{\pi} \tan \left(\frac{\pi}{2} \frac{\phi}{\phi_m} \right).$$

And in particular at the reattachment point, the above becomes

$$\tan \beta_r = \frac{2\phi_m}{\pi} \tan \left(\frac{\pi}{2} \frac{\phi_r}{\phi_m} \right). \quad (6)$$

An expression for the arc distance may also be deduced from Figure 2:

$$d\left(\frac{s}{b}\right) = \left[\left(\frac{r}{b} d\phi \right)^2 + \left(\frac{dr}{b} \right)^2 \right]^{\frac{1}{2}},$$

and consequently,

$$\frac{s}{b} = \int_0^{\phi} \left[\left(\frac{r}{b} \right)^2 + \left(\frac{dr/b}{d\phi} \right)^2 \right]^{\frac{1}{2}} d\phi. \quad (7)$$

Substitution of equations 3 and 5 gives the following result:

$$\frac{s}{b} = \frac{a}{b} \int_0^{\frac{\pi}{2} \frac{\phi}{\phi_m}} \left[1 - \left(1 - \left(\frac{2\phi_m}{\pi} \right)^2 \right) \sin^2 \left(\frac{\pi}{2} \frac{\phi}{\phi_m} \right) \right]^{\frac{1}{2}} d\left(\frac{\pi}{2} \frac{\phi}{\phi_m} \right).$$

Defining $\psi = \frac{\pi}{2} \frac{\phi}{\phi_m}$, the above becomes

$$\frac{s}{a} = \int_0^\psi \left[1 - \left(1 - \left(\frac{2\phi_m}{\pi} \right)^2 \right) \sin^2 \psi \right]^{\frac{1}{2}} d\psi \quad (8)$$

which is an elliptic integral of the second kind. As will be seen in a later section, another expression for arc distance can be derived; and in each of the three cases considered, the expression will be of the form (s/bRe) .

At this point it is a simple task to extract a general solution for the low Reynolds number reattachment problem from the expression for the path,

$$\frac{r}{b} = \frac{a}{b} \sin \left(\frac{\pi}{2} \frac{\phi}{\phi_m} \right). \quad (3)$$

At reattachment, $\phi = \phi_r$ and $r = X_r$. Substituting these symbols as well as the expressions for arc length leaves

$$\frac{X_r}{b} = Re \frac{(s/bRe)}{(s/a)} \sin \left(\frac{\pi}{2} \frac{\phi_r}{\phi_m} \right).$$

And finally setting

$$C_1 = \frac{(s/bRe)}{(s/a)} \sin \left(\frac{\pi}{2} \frac{\phi_r}{\phi_m} \right),$$

the equation for reattachment becomes

$$\frac{X_r}{b} = C_1 Re. \quad (9)$$

It is seen that reattachment distance varies linearly with Reynolds number--a conclusion which has been experimentally verified for low Reynolds number jet reattachment.

Two-Dimensional Laminar Jet Theory

As stated previously, this investigation shall incorporate into the general solution of the reattachment problem three different descriptions of the velocity field of the two-dimensional laminar jet. There follows below a development and discussion of each of the velocity profiles.

1. The Bickley Solution

Since the Bickley formulation appears so often in standard texts (14) and the literature, it is felt that a complete development of the solution is unnecessary. However, a brief outline is presented to provide contrast for comparison with the other solutions.

A number of assumptions are made, and among them are the following. Since the constant pressure of the surroundings impresses itself on the jet, the pressure gradient along the jet length is neglected. Thus the momentum flux J is constant. Also it is assumed that the velocity profiles are similar.

With these assumptions in hand, a stream function is constructed, and the appropriate substitutions are made into the boundary layer equation. With some manipulation, the resulting second order differential equation is put into a form from which it is easily integrated. Therefore the resulting solution is exact, and the

velocity component in the direction of flow may be deduced to be

$$u = 0.4543 \left[\frac{J^2}{\rho^2 v x'} \right]^{1/3} \operatorname{sech}^2 \xi, \quad (10a)$$

where

$$\xi = 0.2752 \left(\frac{J}{\rho v^2} \right)^{1/3} \frac{y}{x'^{2/3}}. \quad (10b)$$

However, the assumption of similar velocity profiles eliminates one of the boundary conditions: a finite jet velocity at the origin. Accordingly, it is seen that the origin is a singular point. The jet velocity is infinite there, and to compensate, one must imagine the jet orifice to be infinitely thin. Thus the solution is encumbered by the necessity of locating a virtual origin.

Comparin (5) attacks the problem by assuming that a uniform velocity profile exists at the nozzle exit. He then establishes that at a distance $\frac{1}{64} \operatorname{Re} b$ downstream from the nozzle, the potential core will have deteriorated. Ignoring any transition region and matching center line velocity with potential velocity at the point of potential core deterioration, Comparin calculates the virtual origin to be a distance of $\frac{5}{64} \operatorname{Re} b$ upstream from the nozzle exit. However if one attacks the problem from the viewpoint of determining that distance from the virtual origin where the calculated mass flow equals that emerging from the nozzle, one finds that the virtual origin lies only a distance of $\frac{1}{36} \operatorname{Re} b$ behind the nozzle exit. Here is the dilemma. Some compromise must be made, and it is quite

evident why the Bickley solution is applicable only at large distances from the origin.

To facilitate future use, equations 10a and 10b may be written in the form

$$\theta_s = \frac{u}{U} = 0.4543 \left(\frac{x'}{\text{Re } b} \right)^{-1/3} \text{sech}^2 \xi \quad (11a)$$

$$\xi = 0.2752 \left(\frac{x'}{\text{Re } b} \right)^{-2/3} \frac{y}{b} \quad (11b)$$

and where

$$\frac{x'}{\text{Re } b} = \frac{x}{\text{Re } b} + \frac{5}{64} \cdot \quad (11c)$$

2. The Okabe Approximate Solution

Okabe attacks the problem of the two-dimensional laminar jet by choosing a function for the velocity component in the flow direction of the form

$$\theta_o = \frac{u}{U} = (1 - e^{-(1-\eta)/\lambda})^3 + \frac{3}{\lambda} e^{-1/\lambda} (1 - e^{-1/\lambda})^2 \eta + a_1 \eta^2 + a_2 \eta^3 + a_3 \eta^4. \quad (12)$$

Okabe has not published the logical processes from which the function emerged, however he intimates that it is a product of the Kármán-Pohlhausen momentum equation. Nevertheless, the function is not as formidable as it would seem; and in fact, it predicts the growth of the laminar jet with great success.

The quantity λ is a function of x only, and as will be seen, it is of the form

$$\lambda \begin{cases} = 0, & x = 0 \\ > 0, & x > 0. \end{cases}$$

Unlike the Bickley formulation, the jet is finitely bounded by the function $y = \pm\Delta$ where Δ is also a function of x . The quantity η is defined to be y/Δ . The coefficients a_1 , a_2 , and a_3 may be determined from the boundary conditions at the edges of the jet. At $\eta = 1$, the function $\theta_o = \theta_o(\lambda, \eta)$ must satisfy

$$\theta_o = \frac{\partial \theta_o}{\partial \eta} = \frac{\partial^2 \theta_o}{\partial \eta^2} = 0.$$

Accordingly, a system of linear equations may be written and the unknowns a_1 , a_2 , and a_3 found:

$$a_1 = -9\Lambda, \quad a_2 = 9\Lambda, \quad a_3 = -3\Lambda,$$

where

$$\Lambda = \frac{\varepsilon(1-\varepsilon)^2}{\lambda} \quad \text{with } \varepsilon = e^{-1/\lambda}.$$

Since it is assumed that the pressure gradient in the direction of flow is negligible, the boundary layer equation at the line of symmetry can be reduced to

$$\left(\theta_o \frac{\partial \theta_o}{\partial x} \right)_{\eta=0} = \left(\frac{v}{U} \frac{\partial^2 \theta_o}{\partial y^2} \right)_{\eta=0}.$$

After evaluation of the various quantities and substitution, the

above yields

$$\frac{dx}{bRe} = \frac{1}{4} \frac{(1-\varepsilon)^4 \delta^2}{6\lambda(1-\varepsilon) + (1-3\varepsilon)} d\lambda$$

where δ is defined to be $2\Delta/b$. After integration it is seen that λ is implicitly defined in the relation

$$\frac{x}{bRe} = \frac{1}{4} \int_0^\lambda \frac{(1-\varepsilon)^4 \delta^2}{6\lambda(1-\varepsilon) + (1-3\varepsilon)} d\lambda. \quad (13)$$

There remains only the task of finding an expression for the dimensionless jet width δ . Because the pressure gradient has been ignored, the momentum flux in the direction of flow is constant:

$$\rho U^2 b = 2\rho \int_0^\Delta u^2 dy.$$

Dividing by the quantity $\rho U^2 b$ and factoring Δ from the integrand yields

$$1 = \frac{2}{b} \Delta \int_0^{\Delta/\Delta} \left(\frac{u}{U}\right)^2 d\left(\frac{y}{\Delta}\right).$$

And finally,

$$\delta = \left[\int_0^1 \theta_o^2 d\eta \right]^{-1}. \quad (14)$$

The integrand is exactly integrable, and the details of the integration may be found in Appendix A.

Unlike Bickley's exact solution, the Okabe approximation is applicable everywhere in the jet flow. No virtual origin is required, because at the origin, the jet emerges from an orifice of width b with a finite and uniform velocity. Also it has been demonstrated by Thomas (15) that agreement between the theoretical and the experimental profiles is quite good. However, one must pay dearly for these benefits. Evaluation of equation 14 is torturous at best, and quadrature methods must be employed to evaluate equation 13. The results of such calculations for a range of the variable λ appear in Table 1.

3. The Modified Okabe Solution

Reference has been made previously to Thomas' article (15) in which an attempt was made to alter the Okabe approximate solution so that the effect of a parabolic velocity profile at the nozzle orifice might be included. Thomas' efforts are judged to be unsuccessful by this author, and criticism of Thomas' method are found in Appendix D. The present effort retains Thomas' modification of the Okabe velocity profile, but there is no subsequent similarity in the two approaches. This new approach is largely patterned after Okabe's.

The modified velocity profile is

$$\theta_m = \frac{u}{U} = \frac{3}{2} \left[(1-\eta^2)(1-\epsilon e^{\eta/\lambda})^3 + 3\Lambda\eta + a_1\eta^2 + a_2\eta^3 + a_3\eta^4 \right] \quad (15)$$

Okabe Velocity Profile

λ	δ	x/bRe
0.0	1.0000	0.0
0.1	1.3242	0.02535
0.2	1.8991	0.05828
0.3	2.8627	0.1108
0.4	4.4222	0.2007
0.5	6.8766	0.3587
0.6	10.629	0.6375
0.7	16.207	1.124
0.8	24.306	1.959
0.9	35.791	3.361
1.0	51.740	5.663

Modified Okabe Velocity Profile

λ	δ	x/bRe
0.0	1.0000	0.0
0.1	1.0512	0.00002750
0.2	1.3082	0.004213
0.3	1.8332	0.02209
0.4	2.7245	0.05853
0.5	4.1426	0.1249
0.6	6.3049	0.2429
0.7	9.5512	0.4499
0.8	14.219	0.8029
0.9	20.498	1.392
1.0	30.825	2.343

Table 1. Approximate solutions for the plane jet

where the symbols ϵ and Λ have been defined previously. Also it is assumed that the pressure gradient in the direction of flow is negligible. Thus at the edges of the jet boundary ($\eta = 1$), all three of the following boundary conditions must be met:

$$\theta_m = \frac{\partial \theta_m}{\partial \eta} = \frac{\partial^2 \theta_m}{\partial \eta^2} = 0.$$

This results in a set of linear equations:

$$\theta_m \Big|_{\eta = 1} = 3\Lambda + a_1 + a_2 + a_3 = 0$$

$$\frac{\partial \theta_m}{\partial \eta} \Big|_{\eta = 1} = 3\Lambda + 2a_1 + 3a_2 + 4a_3 = 0$$

$$\frac{\partial^2 \theta_m}{\partial \eta^2} \Big|_{\eta = 1} = a_1 + 3a_2 + 6a_3 = 0$$

Solving for a_1 , a_2 , and a_3 and substituting into equation 15 leaves

$$\theta_m = \frac{3}{2} \left[(1-\eta^2)(1-\epsilon e^{\eta/\lambda})^3 + 3\Lambda\eta(1-\eta)^3 \right]. \quad (16)$$

It may be easily shown that at $\lambda = 0$,

$$\theta_m \Big|_{\lambda = 0} = \frac{3}{2} (1-\eta^2)$$

which is the desired fully developed profile. Also it may be readily shown that at the axis of symmetry ($\eta = 0$), the following condition is satisfied:

$$\left. \frac{\partial \theta_m}{\partial \eta} \right|_{\eta = 0} = 0.$$

The equation of motion in the x-direction is

$$u \frac{\partial u}{\partial x} + v \frac{\partial u}{\partial y} = -\frac{1}{\rho} \frac{\partial P}{\partial x} + \nu \frac{\partial^2 u}{\partial y^2}.$$

Since $\partial P / \partial x$ is negligible, the equation at the axis of symmetry reduces to

$$u \left. \frac{\partial u}{\partial x} \right|_{y=0} = \nu \left. \frac{\partial^2 u}{\partial y^2} \right|_{y=0}.$$

Dividing by the quantity U^2 ,

$$\theta_m \left. \frac{\partial \theta_m}{\partial x} \right|_{y=0} = \frac{\nu}{U} \left. \frac{\partial^2 \theta_m}{\partial y^2} \right|_{y=0}. \quad (17)$$

But

$$\left. \theta_m \right|_{y=0} = \frac{3}{2} (1-\epsilon)^3,$$

$$\left. \frac{\partial \theta_m}{\partial x} \right|_{y=0} = \left. \frac{\partial \theta_m}{\partial \lambda} \right|_{y=0} \frac{d\lambda}{dx} = -\frac{9}{2} \frac{\Lambda}{\lambda} \frac{d\lambda}{dx},$$

$$\left. \frac{\partial^2 \theta_m}{\partial y^2} \right|_{y=0} = \left. \frac{\partial^2 \theta_m}{\partial \eta^2} \right|_{\eta=0} \frac{1}{\Delta^2} = \frac{3}{2\Delta^2} \left[\frac{6\epsilon^2}{\lambda^2} (1-\epsilon) - \frac{3\epsilon}{\lambda^2} (1-\epsilon)^2 - \frac{18\epsilon}{\lambda} (1-\epsilon)^2 - 2(1-\epsilon)^3 \right].$$

Substituting into equation 17 yields

$$\frac{dx}{bRe} = \frac{9}{8} \frac{\epsilon(1-\epsilon)^4 \delta^2}{3\epsilon[(1-3\epsilon) + 6\lambda(1-\epsilon)] + 2\lambda^2 (1-\epsilon)^2} d\lambda.$$

Integration gives λ implicitly defined by

$$\frac{x}{bRe} = \frac{9}{8} \int_0^\lambda \frac{\epsilon(1-\epsilon)^4 \delta^2}{3\epsilon[(1-3\epsilon) + 6\lambda(1-\epsilon)] + 2\lambda^2 (1-\epsilon)^2} d\lambda. \quad (18)$$

Since the assumption of no pressure gradient implies constant momentum flux,

$$\int_{-\Delta}^{\Delta} \rho u^2 dy \Big|_{\lambda \neq 0} = \int_{-\Delta}^{\Delta} \rho u^2 dy \Big|_{\lambda = 0}.$$

Consequently,

$$2\Delta \int_0^1 \theta_m^2 d\eta \Big|_{\lambda \neq 0} = b \int_0^1 \theta_m^2 d\eta \Big|_{\lambda = 0}.$$

Solving for the dimensionless jet width δ ,

$$\delta = \frac{2\Delta}{b} = \frac{\int_0^1 \frac{9}{4} (1-\eta^2)^2 d\eta}{\int_0^1 \theta_m^2 d\eta}$$

And finally

$$\delta = \frac{6}{5} \left[\int_0^1 \theta_m^2 d\eta \right]^{-1}. \quad (19)$$

The quantity on the right hand side of equation 19 is exactly integrable as may be seen in Appendix A. Equation 18 however requires a quadrature method for its evaluation. The results of such calculations appear in Table 1 along with the original Okabe approximate solution. The velocity profiles of all three solutions--the Bickley, Okabe, and modified Okabe--are compared in Figure 3.

Reattachment Distance Versus Reynolds Number

The analysis is concluded with the substitution of each of the velocity profiles into the general solution for reattachment distance.

1. The Analysis with the Bickley Profile

With substitution of the Bickley velocity profile (equations 11a, b, c) equation 2 becomes

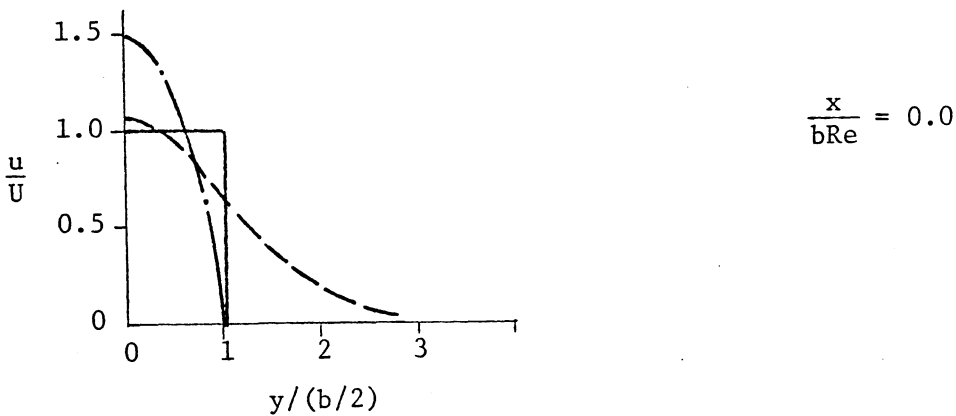
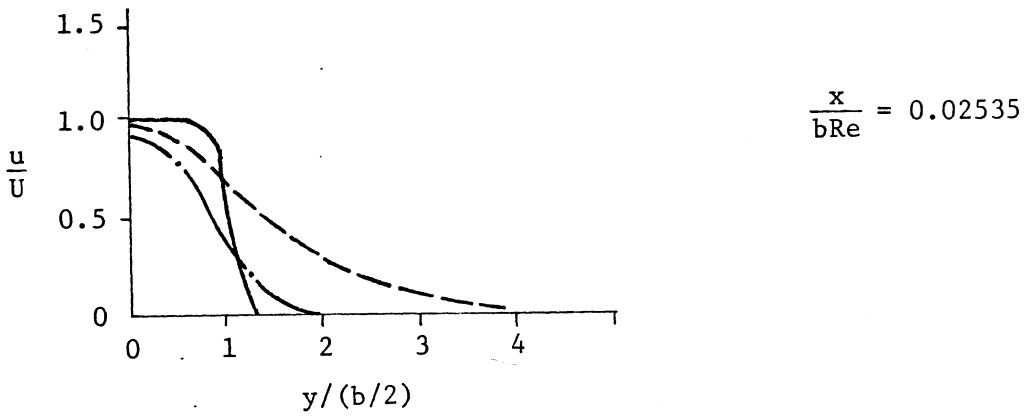
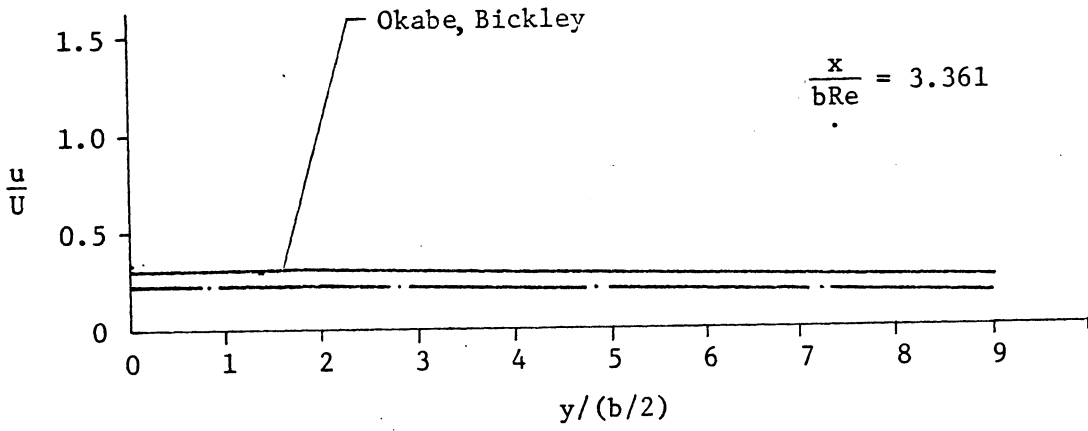


Figure 3. Velocity distributions of the laminar plane jet:
 Bickley (---), Okabe (—), Modified Okabe (-.-)

$$\cos \gamma = \frac{\int_{-\infty}^{y_r} \rho U^2 \theta_s^2 dy - \int_{y_r}^{\infty} \rho U^2 \theta_s^2 dy}{\int_{-\infty}^{\infty} \rho U^2 \theta_s^2 dy} .$$

With simplification this reduces to

$$\cos \gamma = \frac{\int_{-\infty}^{\xi_r} \operatorname{sech}^4 \xi d\xi - \int_{\xi_r}^{\infty} \operatorname{sech}^4 \xi d\xi}{\int_{-\infty}^{\infty} \operatorname{sech}^4 \xi d\xi}$$

and finally to

$$\cos \gamma = \frac{3}{2} \tanh \xi_r - \frac{1}{2} \tanh^3 \xi_r . \quad (20)$$

Since the angle of plate inclination α is known and since it has been established that $\phi_r = \alpha$ and $\gamma = \beta_r$, the angle of reattachment can be determined from equation 6. Equation 20 is merely a third degree polynomial and it is a simple chore to find its roots. By the nature of the hyperbolic tangent, it is known that the desired root lies within (0,1), and Newton's method is perfectly adequate to find the value of the root.

Previously it was determined that the ordinate of the reattaching streamline was given implicitly by

$$b = 2 \int_0^{y_r} \theta \, dy . \quad (1)$$

Substituting equation 11a and adjusting the variable of integration accordingly,

$$1 = \frac{2(0.4543)}{0.2752} \left(\frac{Reb}{x'} \right)^{-1/3} \int_0^{\xi_r} \operatorname{sech}^2 \xi \, d\xi .$$

Solving for the length of the jet path--now denoted by s --in light of equation 11c yields

$$\frac{s}{bRe} = \frac{1}{36 \tanh^3 \xi_r} - \frac{5}{64} . \quad (21)$$

In view of equations 20 and 21, the previous assertion that

$$\lim_{x_r \rightarrow \infty} \cos \gamma = 0$$

is verified.

Thus the solution is complete. The quantity (s/a) is calculated from equation 8 via a quadrature method* and together with the quantity (s/bRe) is substituted into

*The reader may well question the usefulness of employing a quadrature method since tables of elliptic integrals are to be found anywhere. However, because quadrature methods have to be employed elsewhere, it is deemed convenient to apply them here. At any rate, accuracy does not suffer. See Appendix B for details.

$$\frac{Xr}{b} = C_1 Re \quad (9)$$

where

$$C_1 = \frac{(s/bRe)}{(s/a)} \sin\left(\frac{\pi}{2} \frac{\phi_r}{\phi_m}\right).$$

2. The Analysis with the Okabe Profile

The analysis with the Okabe velocity profile is very similar to the previous solution although somewhat less straightforward. Again the development begins with the appropriate substitution into equation 2:

$$\cos \gamma = \frac{\rho \frac{b}{2} U^2 \delta \int_{-1}^{\eta_r} \theta_o^2 d\eta - \rho \frac{b}{2} U^2 \delta \int_{\eta_r}^1 \theta_o^2 d\eta}{\rho b U^2}$$

which readily reduces to

$$\cos \gamma = \frac{1}{2} \delta \left[\int_{-1}^{\eta_r} \theta_o^2 d\eta - \int_{\eta_r}^1 \theta_o^2 d\eta \right].$$

With little effort the above simplifies to

$$\cos \gamma = \delta \int_0^{\eta_r} \theta_o^2 d\eta, \quad (22)$$

where of course $0 \leq \eta_r \leq 1$. The dimensionless jet width δ is given

by equation 14, and the task remains to find the non-dimensional ordinate η_r as a function of the parameter λ .

Accordingly, attention is turned to equation 1:

$$b = 2 \int_0^{y_r} \theta_0 dy .$$

After substitution of the velocity profile, the above may be manipulated so that it appears in the form

$$\eta_r = \int_0^{\eta_r} (3\epsilon e^{\eta/\lambda} - 3\epsilon^2 e^{2\eta/\lambda} + \epsilon^3 e^{3\eta/\lambda}) d\eta - 3\Lambda \int_0^{\eta_r} (\eta - 3\eta^2 + 3\eta^3 - \eta^4) d\eta + \delta^{-1} \quad (23)$$

For any given value of the parameter λ , it is obvious from the physical aspects of the problem that the solution of the above equation exists and is unique. With some confidence in the outcome, the standard fixed point iterative technique is applied:

$$\eta_{r(n+1)} = f(\eta_{r(n)})$$

where n , of course, denotes the number of iterations.

Again from physical intuition, it may be reasoned that as $\lambda \rightarrow \infty$, the ordinate $\eta_r \rightarrow 0$. This can be rigorously proven at this point, but such steps are sacrificed for the sake of brevity. In this spirit, the assertion is made that as $\lambda \rightarrow \infty$ the integral in

equation 22 goes to zero faster than the non-dimensional jet width increases. Thus it is seen from equation 22 that

$$\lim_{X_r \rightarrow \infty} \cos \gamma = 0$$

and moreover that $\cos \gamma$ approaches zero strictly monotonically.

At this juncture it may be wise to bring the analysis into sharper focus. It has been shown that the angle of jet reattachment may be determined strictly from the geometry of the reattachment problem:

$$\gamma = \beta_r = \tan^{-1} \left[\frac{2\phi_m}{\pi} \tan \left(\frac{\pi}{2} \frac{\phi_r}{\phi_m} \right) \right] \quad (6)$$

with $\phi_r = \alpha$. The momentum principle (equation 22) and the continuity concept (equation 23) are introduced in order to determine that value of the parameter λ which corresponds to a given plate angle. The comments in the previous paragraph not only support the proposal for the path of the jet (equation 3) but indicate that for any plate angle there exists a unique λ . This is important not for what it says (the physically obvious: for a given Re and α , reattachment occurs at only one point) but for what it suggests: a method for determining the parameter λ .

The procedure for the calculation of λ is as follows. An initial value of the parameter is assumed such that the corresponding value for $\cos \gamma$, which is calculated from equations 14, 22, and 23,

is less than $\cos \beta_r$ determined from equation 6. Then the subsequent values of λ are diminished by the rule

$$\lambda_{(n)} = \lambda_{(n-1)} - 10^{-L}$$

(where initially $L = 1$) until upon the K^{th} step $\cos \gamma$ first exceeds $\cos \beta_r$. Then the entire process is repeated with the initial value for the parameter chosen to be $\lambda_{(K-1)}$ and with the exponent L augmented by one. Single precision on the IBM 360 computer is quite sufficient for the processes described, and the calculation is terminated when the exponent L exceeds six. Thus the unique value of the parameter λ corresponding to a given plate angle is known to at least the fifth decimal place.

Now that the parameter λ can be found for any given plate inclination, the quantity (s/bRe) can be calculated from

$$\frac{s}{bRe} = \frac{1}{4} \int_0^\lambda \frac{(1-\epsilon)^4 \delta^2}{6\lambda(1-\epsilon) + (1-3\epsilon)} d\lambda. \quad (13)$$

The anti-derivative of the integrand of course does not exist, and numerical integration is required. The Gaussian quadrature method has been chosen for two reasons. As the reader may appreciate, the evaluation of the integrand is a rather lengthy procedure incurring significant computer expense. Therefore, an efficient quadrature is desired. The chosen method is superior to more ordinary ones (e.g. trapezoidal, Simpson's rule) because its n

ordinates are comparable in effectiveness to $2n$ equidistant ordinates*. The second reason for the choice is that if it were desired that the error of the quadrature be known, only the first derivative of the integrand need be found**

As in the analysis with the Bickley solution, the quantity (s/a) is calculated using the Gaussian quadrature method on the elliptic integral of equation 8. Quadrature has been employed at this step to instill a modest degree of flexibility into the analysis. Details of this and the preceding numerical integration are to be found in Appendix B.

Having determined the two expressions for the arc length of the jet, one merely substitutes these quantities into the following equation to complete the analysis:

$$\frac{X_r}{b} = C_1 \operatorname{Re} \quad (9)$$

where

$$C_1 = \frac{(s/b\operatorname{Re})}{(s/a)} \sin \left(\frac{\pi}{2} \frac{\phi_r}{\phi_m} \right).$$

3. The Analysis with the Modified Okabe Profile

The analysis with the modified Okabe velocity profile is much like the previous one. The main difficulty is again the evaluation

* Lanczos, C., Applied Analysis, Prentice Hall, Inc., Englewood Cliffs, N. J., 1956, p. 403, 404.

** Ibid.

of that value of the parameter λ which corresponds to a given plate inclination. Substitution of the appropriate profile into equation 2 yields

$$\cos \gamma = \frac{\rho \frac{b}{2} U^2 \delta \int_{-1}^{\eta_r} \theta_m^2 d\eta - \rho \frac{b}{2} U^2 \delta \int_{\eta_r}^1 \theta_m^2 d\eta}{\frac{6}{5} \rho b U^2} .$$

This can be reduced to

$$\cos \gamma = \frac{5}{6} \delta \int_0^{\eta_r} \theta_m^2 d\eta . \quad (24)$$

The non-dimensional ordinate of the reattaching streamline η_r may be calculated for any given value of the parameter λ from

$$b = 2 \int_0^{y_r} \theta_m dy . \quad (1)$$

After substitution for θ_m and expansion of the integrand, the following results:

$$\begin{aligned} \eta_r &= \int_0^{\eta_r} (3\epsilon e^{\eta/\lambda} - 3\epsilon^2 e^{2\eta/\lambda} + \epsilon^3 e^{3\eta/\lambda}) d\eta \\ &+ \int_0^{\eta_r} (\eta^2 - 3\epsilon \eta^2 e^{\eta/\lambda} + 3\epsilon^2 \eta^2 e^{2\eta/\lambda} - \epsilon^3 \eta^2 e^{3\eta/\lambda}) d\eta \\ &+ 3\lambda \int_0^{\eta_r} (-\eta + 3\eta^2 - 3\eta^3 + \eta^4) d\eta + \frac{2}{3} \delta^{-1} . \quad (25) \end{aligned}$$

This can be solved using the fixed point iteration

$$\eta_{r(n+1)} = f\left(\eta_{r(n)}\right)$$

where n denotes the number of iterations. It can be demonstrated at this point that $\eta_r \rightarrow 0$ as $\lambda \rightarrow \infty$.

Depending on intuitive arguments once again, it may be deduced from equation 24 that

$$\lim_{X_r \rightarrow \infty} \cos \gamma = 0 .$$

The assertion is also made that $\cos \gamma$ approaches zero strictly monotonically. With these assertions in hand, one computes the unique value of the parameter λ corresponding to a given plate angle α in precisely the same manner as before.

Once the value of λ is found, the quantities $(s/b\text{Re})$ and (s/a) may be evaluated from equations 18 and 8 via the Gaussian quadrature method. Details can be found in Appendix B. Substitution into equation 9 yields the desired result:

$$\frac{X_r}{b} = C_1 \text{Re}$$

where

$$C_1 = \frac{(s/b\text{Re})}{(s/a)} \sin \left(\frac{\pi}{2} \frac{\phi_r}{\phi_m} \right) .$$

IV. RESULTS

The analysis of the problem of laminar jet reattachment to an inclined flat plate reduces to

$$\frac{X_r}{b} = C_1 \text{ Re}, \quad (9)$$

where

$$C_1 = \frac{(s/b\text{Re})}{(s/a)} \sin\left(\frac{\pi}{2} \frac{\phi}{\phi_m}\right),$$

for each of the velocity profiles considered. It is obvious that this theory predicts that reattachment distance is directly proportional to Reynolds number for a given plate inclination. How does the theory compare with experiment?

Although experimental data of laminar jet reattachment with sufficiently high aspect ratio to approximate two-dimensional flow are not abundant, Jenkins' measurements (6) show that reattachment distance varies linearly with Reynolds number at least at moderate angles of plate inclination: 25-40 degrees. As the extreme plate inclination (60°) is approached, the data behave somewhat erratically. These trends may be observed in Figures 4-7. A least-squares line has been fitted to each set of data to qualitatively aid in the description of the reattachment phenomenon. Another trend may be deduced from the lines: the slope of the least-squares line increases with increasing plate inclination. On the other hand, the ordinate intercept does not behave in a consistent manner.

For these reasons it is the opinion of this author that equation 9 might adequately describe events as they are. At a plate

inclination of 25 degrees, reattachment distance (measured over the broadest range of Reynolds number) is directly proportional to Reynolds number. This is not the case at plate angles of 30 and 40 degrees. However, data collected at these angles contain no measurements in the range of Reynolds number less than 180 and 110 respectively. Therefore, the dearth of data at high aspect ratios allows one to interpret the least-squares "fit" only in a qualitative sense; and one need not be too concerned whether the theory (equation 9) provides for an ordinate intercept.

Despite the preceding arguments, the results of the calculations using the Bickley, Okabe, and modified Okabe velocity profiles are most disappointing. The results are tabulated in Table 2 and are compared with Jenkins' data in Figures 4-7. The computer programs may be found in Appendix C. Only at an angle of inclination of 30 degrees does the theory bear some semblance to experiment. Very gross discrepancies between theory and experimental fact occur at all other plate inclinations.

The differences among the three analyses are quite evident. The modification of the Okabe approximate solution to include the effect of an initially fully developed laminar jet is significant. Theoretically this effect is of the first order as it diminishes the constant of proportionality C_1 of the Okabe analysis sharply for all plate inclinations. It should be noted that subsequent measurements by Ricketts (10) reveal that the laminar jet studied by Jenkins might be considered to be fully developed.*

*The disruptive effects of vena contracta were detected as well.

	Plate Inclination				
	20°	25°	30°	40°	50°
C_1 , Bickley	-0.0194	-0.00226	0.0248	0.170	1.36
C_1 , Okabe	0.0398	0.0619	0.0954	0.256	1.44
C_1 , Modified Okabe	0.0249	0.0401	0.0640	0.187	1.23

Table 2. The proportionality constant C_1 for various plate inclinations

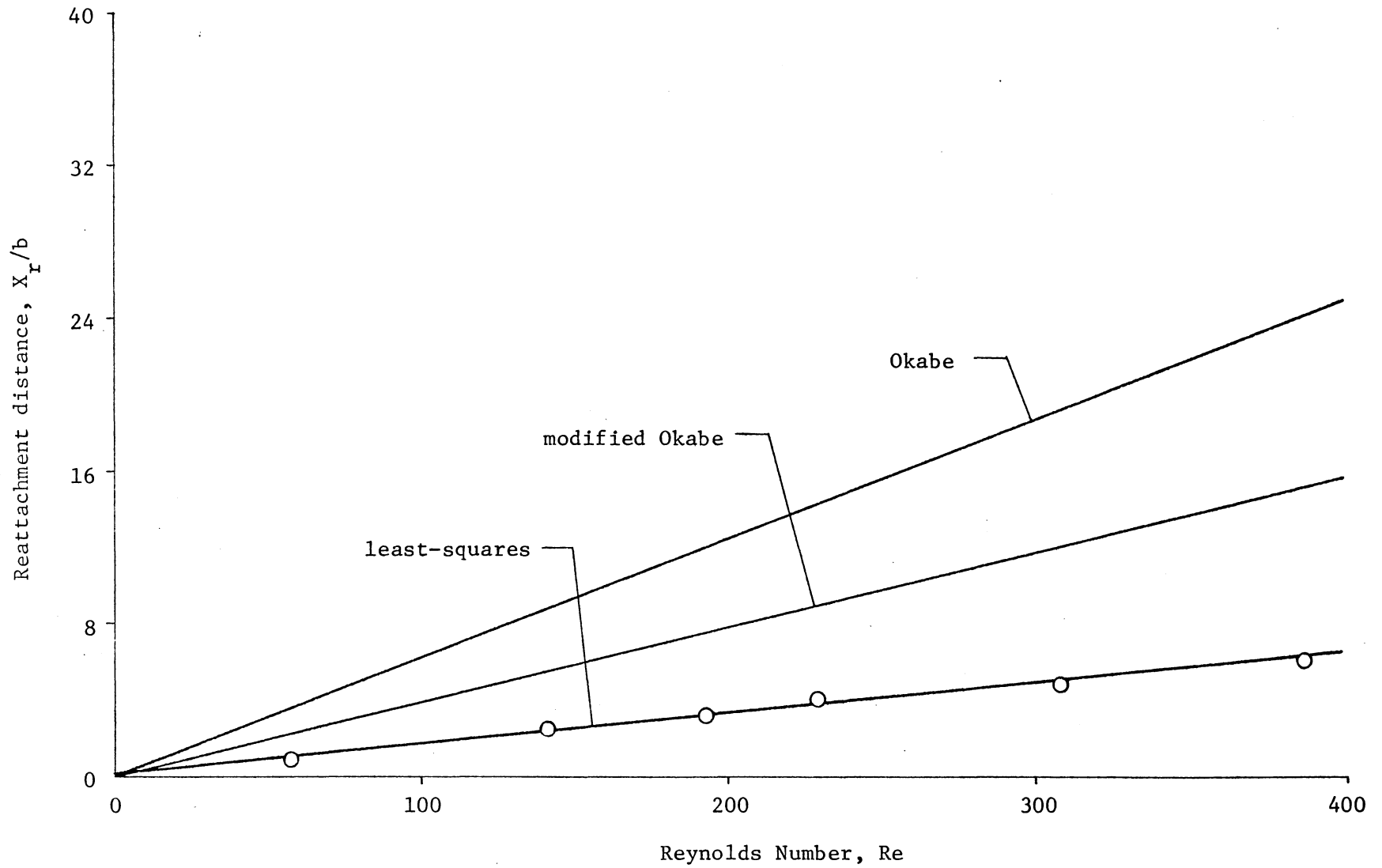


Figure 4. Laminar jet reattachment to a flat plate inclined at 25°

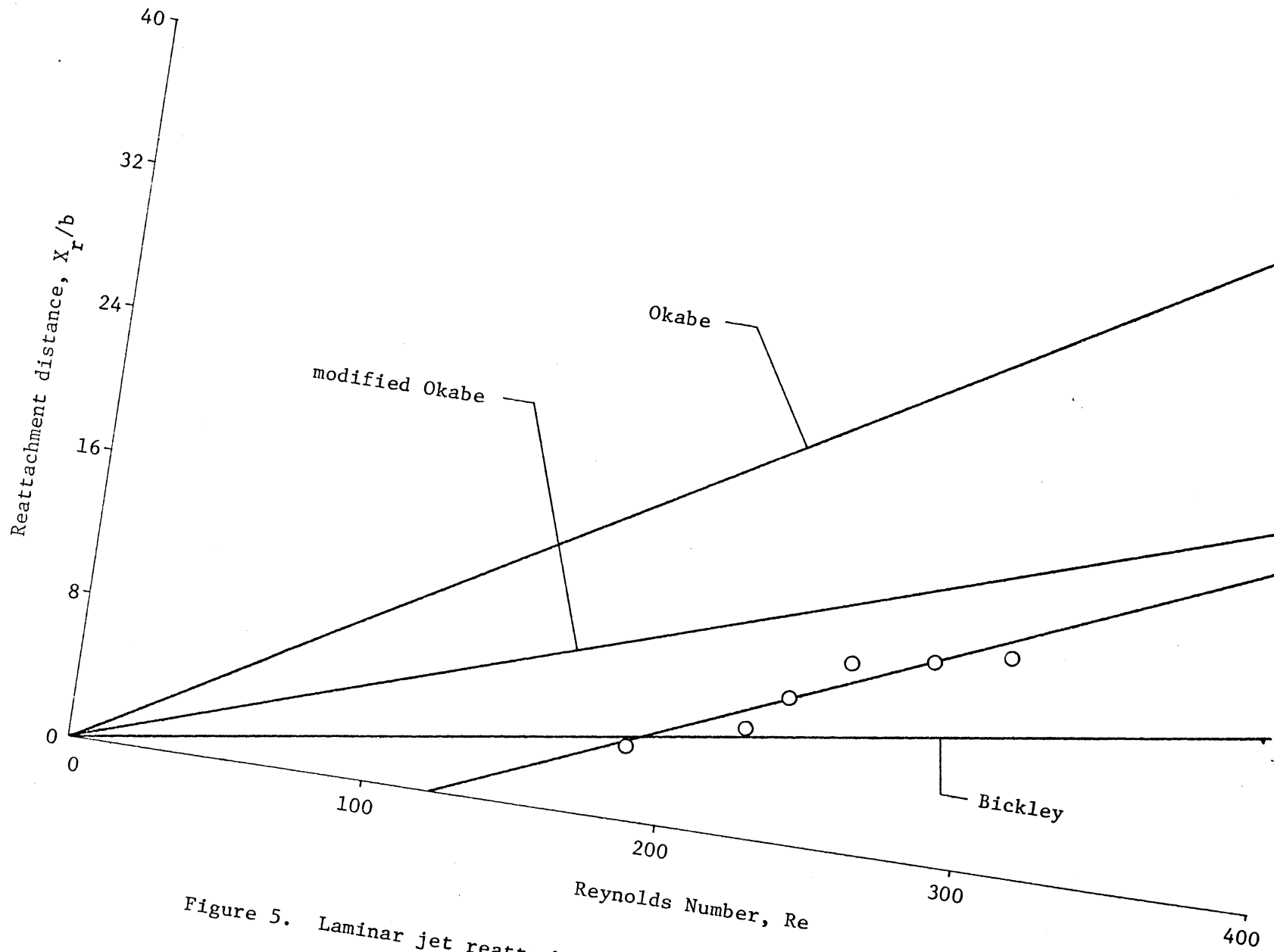


Figure 5. Laminar jet reattachment to a flat plate inclined at 30°

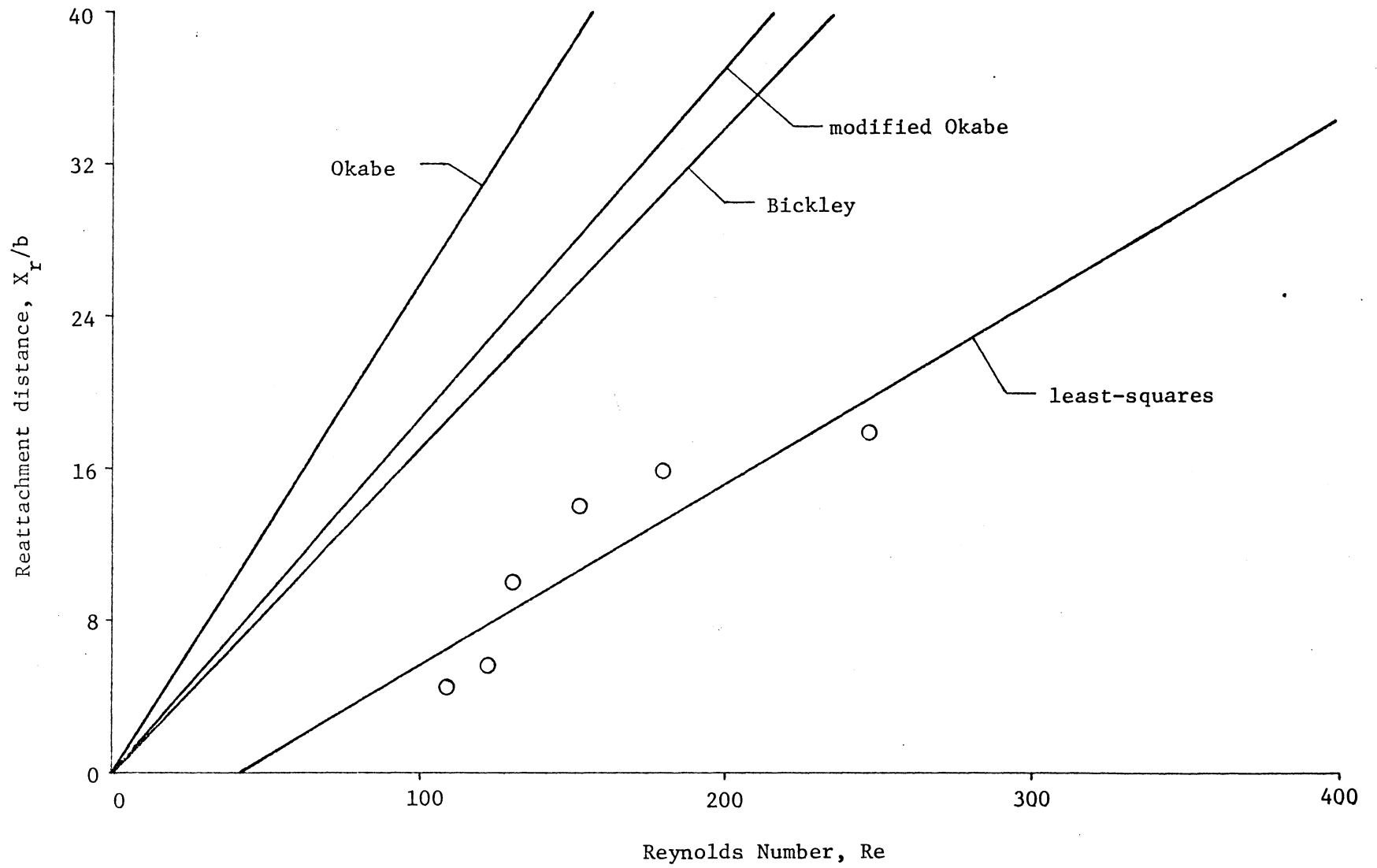


Figure 6. Laminar jet reattachment to a flat plate inclined at 40°

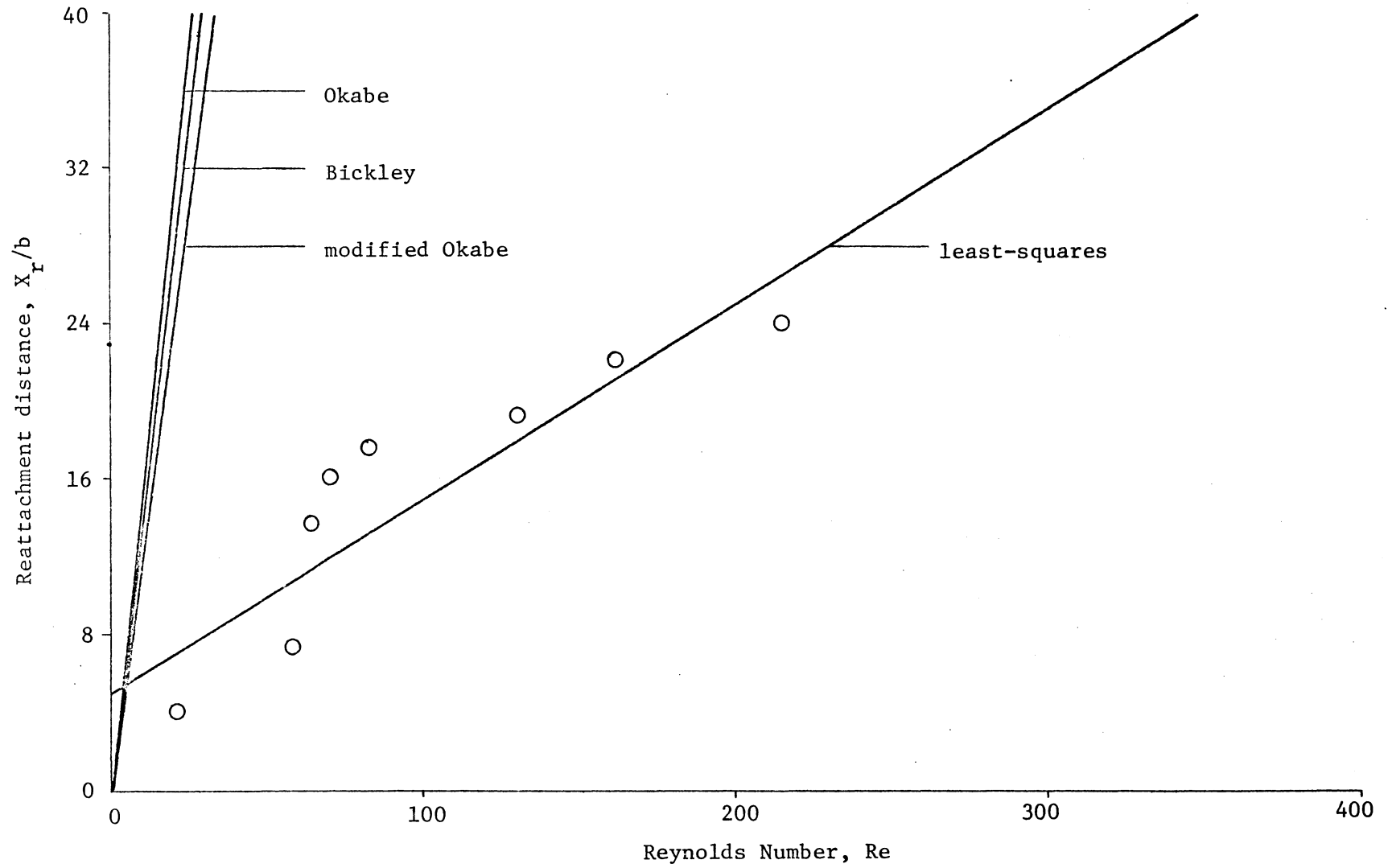


Figure 7. Laminar jet reattachment to a flat plate inclined at 50°

The disparity between the analyses using the Bickley and Okabe velocity profiles may be disturbing. However, one must remember that the choice of a virtual origin for the Bickley formulation was arbitrary to some extent. By choosing another virtual origin (e.g., by satisfying mass conservation at the orifice), better agreement with the Okabe analysis can be achieved commensurately with poorer correlation with the experimental data. It is apparent from Figures 4-7, however, that as the maximum plate inclination is approached, the differences among all three analyses become less significant. This is in harmony with intuition--at the maximum plate inclination reattachment distance is infinite and thus independent of the properties of the laminar jet.

The task remains to account for the large discrepancies between theory and experiment. Referring to the list of assumptions implicit to the general solution of the reattachment problem, one must conclude that the order of the error introduced by several of the assumptions is unknown. Assumptions ii, iii, and vi as yet have not been studied analytically or experimentally. On the other hand, Sawyer's measurements (11) on a turbulent jet near reattachment show the validity of assumption v.

On account of these arguments, the most vulnerable point in the analysis has been the application of Newton's second law about the reattachment point (equation 2). In order to judge the sensitivity of this calculation to induced error, the cosine of the reattachment angle for the Okabe analysis (equation 22) was

adjusted by a factor of 5/6. This had the result of diminishing the proportionality constant C_1 to values below corresponding ones of the modified Okabe approach. That is, there resulted net changes in C_1 sometimes exceeding 30%.

The present theory is rather attractive on paper when compared to previous efforts with the problem of laminar jet reattachment. The increasing curvature of the reattaching streamline is treated in the analysis as well as the initial state of development of the jet. Unfortunately these advantages are not realized. The expression for the cosine of the reattachment angle (equation 2) produces results which are too sensitive to error inherent in equation 2. Although the analysis yields an analytical insight to the effect of initial jet development on reattachment, the theory fails in its primary purpose--the precise determination of jet reattachment distance as a function of Reynolds number for low Reynolds number flows.

V. ACKNOWLEDGEMENTS

I wish to express my gratitude to the members of the advisory committee: Dr. R. A. Comparin, Chairman, Dr. J. B. Jones, and Dr. F. J. Pierce. Their advice and criticism both in and out of the classroom have been highly valued by me. In this regard I extend very special thanks to Dr. Jones and to Dr. Comparin, who have been extremely generous with their counsel over the last few years.

On a more intimate level I can only note here my indebtedness to my family and to my bride Christa.

VI. BIBLIOGRAPHY

1. da C. Andrade, E. N., "The Velocity Distribution in a Liquid-into-Liquid Jet. Part 2: The Plane Jet," The Proceedings of the Physical Society, vol. 51, part 5, no. 287, September 1939, pp. 784-793.
2. Bickley, W. G., "The Plane Jet," Philosophical Magazine, 7th series, vol. 23, April 1937, pp. 727-731.
3. Bourque, C., "Reattachment of a Two-Dimensional Jet to an Adjacent Flat Plate," Advances in Fluidics, ASME, 1967, pp. 192-204.
4. Bourque, C. and Newman, B. G., "Reattachment of a Two-Dimensional Jet to an Adjacent Flat Plate," The Aeronautical Quarterly, vol. 11, August 1960, pp. 201-232.
5. Comparin, R. A., Jenkins, W. C., and Moore, R. B., "Jet Reattachment at Low Reynolds Numbers and Moderate Aspect Ratios," ASME Paper No. 67-FE-25.
6. Jenkins, W. C., "Effect of Reynolds Number and Aspect Ratio on Jet Reattachment," M.S. Thesis, Blacksburg: Virginia Polytechnic Institute, December 1966.
7. Moore, R. B., "Jet Reattachment to an Inclined Wall at Low Reynolds Number," M.S. Thesis, Blacksburg: Virginia Polytechnic Institute, September 1965.
8. Okabe, J., "Approximate Calculations of Laminar Jets (continued)," Reports of the Research Institute for Fluid Engineering, Kyushu University, vol. 5, no. 1, September 1948, pp. 15-22.

9. Okabe, J., "Approximate Calculations of Laminar Jets (Supplementary Note)," Reports of the Research Institute for Applied Mechanics, Kyushu University, vol. 4, no. 13, July 1955, pp. 23-27.
10. Ricketts, G. B., "An Experimental Investigation of a Two-Dimensional Laminar Jet Near the Nozzle Exit," M.S. Thesis, Blacksburg: Virginia Polytechnic Institute, May 1968.
11. Sawyer, R. A., "The Flow due to a Two-Dimensional Jet Issuing Parallel to a Flat Plate," Journal of Fluid Mechanics, vol. 9, part 4, December 1960, pp. 543-560.
12. Sawyer, R. A., "Two-Dimensional Reattaching Jet Flows Including the Effects of Curvature on Entrainment," Journal of Fluid Mechanics, vol. 17, part 4, December 1963, pp. 481-498.
13. Schlichting, H., "Laminare Strahlausbreitung," Zeitschrift für Angewandte Mathematik und Mechanik, bd. 13, August 1933, pp. 260-263.
14. Schlichting, H., Boundary Layer Theory, fourth edition, McGraw-Hill Book Company, Inc., New York, N. Y., 1960, pp. 164-168.
15. Thomas, A. L., "Force and Mass Balances of the Incompressible, Isothermal, Planar Laminar Jet Issuing from a Finite Source," Chemical Engineering Science, vol. 8, 1958, pp. 254-264.

**The vita has been removed from
the scanned document**

Appendix A

Integration of the Square of the Velocity Functions of the Okabe and Modified Okabe Solutions

Although the Okabe and modified Okabe velocity functions (equations 12 and 15) are rather formidable in appearance, mathematical operations on these functions proceed straightforwardly if a systematic approach is used. As is demonstrated in parts 1 and 2 of this appendix, the squares of the velocity functions may be integrated over an interval of the variable η exactly. However, for reasons of which the reader shall be made aware, it has been decided not to carry the evaluation of these integrals to their conclusion by hand. Thus, two functions subprograms have been written which assume most of the burden of computation. These subprograms are explained in part 3.

1. Evaluation of $\int_s^t \theta_o^2 d\eta$ where $0 \leq s, t \leq 1$

The velocity function of the Okabe approximate solution is

$$\theta_o(\lambda, \eta) = (1 - \epsilon e^{\eta/\lambda})^3 + 3\Lambda \eta(1-\eta)^3$$

Squaring the function gives

$$\theta_o^2 = (1 - \epsilon e^{\eta/\lambda})^6 + 6\Lambda (1 - \epsilon e^{\eta/\lambda})^3 \eta(1-\eta)^3 + 9\Lambda^2 \eta^2(1-\eta)^6.$$

Expanding and integrating over $s \leq \eta \leq t$,

$$\begin{aligned}
 & \int_s^t \theta_0^2 d\eta = \\
 & \int_s^t (1 - 6\epsilon e^{\eta/\lambda} + 15\epsilon^2 e^{2\eta/\lambda} - 20\epsilon^3 e^{3\eta/\lambda} + 15\epsilon^4 e^{4\eta/\lambda} - 6\epsilon^5 e^{5\eta/\lambda} + \epsilon^6 e^{6\eta/\lambda}) d\eta \\
 & \qquad \qquad \qquad \text{BINT (1)} \\
 & + 6\lambda \left[\int_s^t \eta (1 - 3\epsilon e^{\eta/\lambda} + 3\epsilon^2 e^{2\eta/\lambda} - \epsilon^3 e^{3\eta/\lambda}) d\eta \right. \\
 & \qquad \qquad \qquad \text{SINT (1)} \\
 & - 3 \int_s^t \eta^2 (1 - 3\epsilon e^{\eta/\lambda} + 3\epsilon^2 e^{2\eta/\lambda} - \epsilon^3 e^{3\eta/\lambda}) d\eta \\
 & \qquad \qquad \qquad \text{SINT (2)} \\
 & + 3 \int_s^t \eta^3 (1 - 3\epsilon e^{\eta/\lambda} + 3\epsilon^2 e^{2\eta/\lambda} - \epsilon^3 e^{3\eta/\lambda}) d\eta \\
 & \qquad \qquad \qquad \text{SINT (3)} \\
 & \left. - \int_s^t \eta^4 (1 - 3\epsilon e^{\eta/\lambda} + 3\epsilon^2 e^{2\eta/\lambda} - \epsilon^3 e^{3\eta/\lambda}) d\eta \right] \\
 & + 9\lambda^2 \int_s^t (\eta^2 - 6\eta^3 + 15\eta^4 - 20\eta^5 + 15\eta^6 - 6\eta^7 + \eta^8) d\eta \cdot \qquad (1A) \\
 & \qquad \qquad \qquad \text{BINT (3)}
 \end{aligned}$$

The labels appearing underneath the terms in the equation refer to variable names used in the computer programs. It is seen that each of the above integrals can be quickly reduced to a sum of smaller integrals, each of which has one of the following forms:

$$i) \int x^n dx, \text{ where } n \geq 0$$

$$ii) \int x^n e^{ax} dx, \text{ where } n \geq 0.$$

The anti-derivatives of forms i and ii exist, of course, and it is a simple task to program the digital computer to perform these rather tiresome calculations.

$$2. \text{ Evaluation of } \int_s^t \theta_m^2 d\eta \text{ where } 0 \leq s, t \leq 1$$

The velocity function of the modified Okabe approximate solution is

$$\theta_m(\lambda, \eta) = \frac{3}{2} \left[(1-\eta^2)(1-\epsilon e^{\eta/\lambda})^3 + 3\Lambda\eta(1-\eta)^3 \right]$$

Squaring the function gives

$$\theta_m^2 = \frac{9}{4} \left[(1-\eta^2)^2 (1-\epsilon e^{\eta/\lambda})^6 + 6\Lambda\eta(1-\eta^2)(1-\eta)^3 (1-\epsilon e^{\eta/\lambda})^3 + 9\Lambda^2 \eta^2 (1-\eta)^6 \right]$$

Expanding and integrating over $s \leq \eta \leq t$,

$$\int_s^t \theta_m^2 d\eta =$$

$$\frac{9}{4} \left[\int_s^t (1-6\epsilon e^{\eta/\lambda} + 15\epsilon^2 e^{2\eta/\lambda} - 20\epsilon^3 e^{3\eta/\lambda} + 15\epsilon^4 e^{4\eta/\lambda} - 6\epsilon^5 e^{5\eta/\lambda} + \epsilon^6 e^{6\eta/\lambda}) d\eta \right]$$

SINT (1)

$$- 2 \int_s^t \eta^2 (1-6\epsilon e^{\eta/\lambda} + 15\epsilon^2 e^{2\eta/\lambda} - 20\epsilon^3 e^{3\eta/\lambda} + 15\epsilon^4 e^{4\eta/\lambda} - 6\epsilon^5 e^{5\eta/\lambda} + \epsilon^6 e^{6\eta/\lambda}) d\eta$$

SINT (2)

$$+ \left. \int_s^t n^4 (1 - 6\epsilon e^{n/\lambda} + 15\epsilon^2 e^{2n/\lambda} - 20\epsilon^3 e^{3n/\lambda} + 15\epsilon^4 e^{4n/\lambda} - 6\epsilon^5 e^{5n/\lambda} + \epsilon^6 e^{6n/\lambda}) dn \right] \quad \text{SINT (3)}$$

$$+ 6\Lambda \frac{9}{4} \left[\int_s^t n (1 - 3\epsilon e^{n/\lambda} + 3\epsilon^2 e^{2n/\lambda} - \epsilon^3 e^{3n/\lambda}) dn \right] \quad \text{SINT (4)}$$

$$- 3 \int_s^t n^2 (1 - 3\epsilon e^{n/\lambda} + 3\epsilon^2 e^{2n/\lambda} - \epsilon^3 e^{3n/\lambda}) dn \quad \text{SINT (5)}$$

$$+ 2 \int_s^t n^3 (1 - 3\epsilon e^{n/\lambda} + 3\epsilon^2 e^{2n/\lambda} - \epsilon^3 e^{3n/\lambda}) dn \quad \text{SINT (6)}$$

$$+ 2 \int_s^t n^4 (1 - 3\epsilon e^{n/\lambda} + 2\epsilon^2 e^{2n/\lambda} - \epsilon^3 e^{3n/\lambda}) dn \quad \text{SINT (7)}$$

$$- 3 \int_s^t n^5 (1 - 3\epsilon e^{n/\lambda} + 3\epsilon^2 e^{2n/\lambda} - \epsilon^3 e^{3n/\lambda}) dn \quad \text{SINT (8)}$$

$$+ \left[\int_s^t n^6 (1 - 3\epsilon e^{n/\lambda} + 3\epsilon^2 e^{2n/\lambda} - \epsilon^3 e^{3n/\lambda}) dn \right] \quad \text{SINT (9)}$$

$$+ 9\Lambda^2 \frac{9}{4} \int_s^t (n^2 - 6n^3 + 15n^4 - 20n^5 + 15n^6 - 6n^7 + n^8) dn. \quad \text{(2A)}$$

BINT (3)

Again it can be seen that each of the above integrals can be reduced to a sum of smaller integrals, each of which is either of form i or ii.

3. Integration of Forms i and ii

The anti-derivatives of forms i and ii exist, and they are the following:

$$i) \int x^n dx = \frac{1}{n+1} x^{n+1}, \text{ where } n \geq 0$$

$$ii) \int x^n e^{ax} dx = e^{ax} \left[\frac{x^n}{a} - \frac{n x^{n-1}}{a^2} + \frac{n(n-1)x^{n-2}}{a^3} - \dots \right. \\ \left. \dots + (-1)^{n-1} \frac{n! x}{a^n} + (-1)^n \frac{n!}{a^{n+1}} \right], \text{ where } n \geq 0.$$

Form i is straightforward and requires no further comment. However, form ii deserves some attention. It is seen that the finite series may be written more compactly as

$$\int x^n e^{ax} dx = e^{ax} \sum_{k=1}^{n+1} (-1)^{k-1} \frac{n!}{(n-k+1)!} \frac{x^{n-k+1}}{a^k}, \text{ where } n \geq 0.$$

Also an examination of equations 1A and 2A reveals that every exponential term occurs in the form

$$e^m e^{m\eta/\lambda}$$

where m is an integer. Therefore, the accuracy of the calculation is enhanced by retaining the constant coefficient

$$\epsilon^m = e^{-m/\lambda}$$

in the integrand.

Unfortunately, the problem of exponential underflow occurs when the above calculations (form ii) are performed for values of the parameter λ less than 0.035. However, the only computations which are affected are in the evaluation of equations 13 and 18 by numerical procedures.

It should also be mentioned that the integral forms i and ii occur frequently in the calculation of the reattaching streamline for both profiles; and the appropriate subprograms have been used accordingly.

Appendix B

Application of the Gaussian Quadrature Method

It is not the purpose of this section to present mathematical discussion of the well-known Gaussian quadrature method but rather to outline its application in the present work. The method has been used successfully in the evaluation of equations 8, 13, and 18, and each application will be dealt with separately.

1. Evaluation of Equation 8

This equation is an elliptic integral of the second kind, which has the form

$$A = \int_0^{\phi} (1 - k^2 \sin^2 \phi)^{1/2} d\phi. \quad (1B)$$

Making the substitution $x = \sin \phi$, the above quickly reduces to

$$A = \int_0^{x_{\max}} \frac{\sqrt{1 - k^2 x^2}}{\sqrt{1 - x^2}} dx. \quad (2B)$$

The point $x = 1$ is singular, and thus one must expect the quadrature method to fail as the argument ϕ approaches 90 degrees.

To apply the Gaussian quadrature, it is necessary to shift the interval of integration from $[0, x_{\max}]$ to $[-1, 1]$. This is done by the following transformation of variable:

$$x = \frac{x_{\max}}{2} (\psi + 1). \quad (3B)$$

Then denoting the integrand of equation (2B) by y , one sees that

$$y = y(x) = y(\psi)$$

and finally that

$$A = \int_0^{x_{\max}} y(x) dx = \frac{x_{\max}}{2} \int_{-1}^{+1} y(\psi) d\psi.$$

Finally, it has been determined by the author that sixteen ordinates are quite sufficient to insure at least four significant digit accuracy for all values of the argument k and for values of the argument ϕ not exceeding 81 degrees. Thus we have

$$A \cong \bar{A} = \frac{x_{\max}}{2} \sum_{i=1}^{16} y(\psi_i) w_i$$

where ψ_i and w_i denote the abscissas and weights of the Gaussian quadrature*.

2. Evaluation of Equation 13

The evaluation of equation 13,

$$\frac{x}{bRe} = \frac{1}{4} \int_0^{\lambda_{\max}} \frac{(1-\epsilon)^4 \delta^2}{6\lambda(1-\epsilon) + (1-3\epsilon)} d\lambda,$$

follows exactly as the previous one with only one minor complication.

Although the function in the integrand of the equation is well behaved,

*Davis, P., and Rabinowitz, P., "Abcissas and Weights for Gaussian Quadratures of High Order," Journal of Research of the National Bureau of Standards, vol. 56, no. 1, January 1956, pp. 35-37.

it can not be calculated at values of the parameter λ less than 0.035 without incurring underflow problems with the digital computer. As discussed in Appendix A, underflow will occur during the evaluation of the dimensionless jet width δ at small values of λ . Therefore, when it is required to calculate the value of δ for $\lambda < 0.035$, a linear interpolation is used. This, of course, adds to the error inherent in any quadrature method.

Denoting the integrand of equation 13 by y and making the transformation

$$\lambda = \frac{\lambda_{\max}}{2} (\psi+1), \quad (4B)$$

it is seen that

$$y = y(\lambda) = y(\psi).$$

Then,

$$A = \int_0^{\lambda_{\max}} y(\lambda) d\lambda = \frac{\lambda_{\max}}{2} \int_{-1}^{+1} y(\psi) d\psi$$

and again it follows that

$$A \cong \bar{A} = \frac{\lambda_{\max}}{2} \sum_{i=1}^{16} y(\psi_i) w_i .$$

It has been determined that sixteen ordinates are sufficient to insure convergence. Several trial calculations have been performed using forty-eight ordinates, and the results differ from the present

calculations in only the seventh significant digit. Therefore, the error inherent in the quadrature method is judged to be quite acceptable.

3. Evaluation of Equation 18

The evaluation of this equation,

$$\frac{x}{bRe} = \frac{9}{8} \int_0^{\lambda_{\max}} \frac{\varepsilon(1-\varepsilon)^4 \delta^2}{3\varepsilon[(1-3\varepsilon) + 6\lambda(1-\varepsilon)] + 2\lambda^2 (1-\varepsilon)^2} d\lambda ,$$

by the Gaussian quadrature method proceeds as the previous one.

Again the integrand is a well behaved function, however underflow problems with the digital computer are incurred during the calculation of the dimensionless jet width δ at values of the parameter λ less than 0.038. As before, a linear interpolation is used to calculate δ for $\lambda < 0.038$.

Denoting the integrand by y and making the transformation of variable

$$\lambda = \frac{\lambda_{\max}}{2} (\psi+1) ,$$

it is seen that

$$y = y(\lambda) = y(\psi) .$$

Then,

$$A = \int_0^{\lambda_{\max}} y(\lambda) d\lambda = \frac{\lambda_{\max}}{2} \int_{-1}^{+1} y(\psi) d\psi ,$$

and it follows that

$$A \approx \bar{A} = \frac{\max}{2} \sum_{i=1}^{16} y(\psi_i) w_i .$$

Trial calculations with forty-eight ordinates have been performed, and again no significant differences are evident when these calculations are compared to those with sixteen ordinates.

Appendix C

Computer Programs

In this appendix are presented the computer programs which have been used to determine reattachment distance as a function of Reynolds number for two-dimensional low Reynolds number flows. An IBM 360 digital computer has been used exclusively; and the programs are written in the Fortran IV language. Since the programs are all relatively short, they have been executed in the WATFOR mode. The reader may notice that in the subprograms dealing with the Gaussian quadrature method, the abscissas and weights of the quadrature are in the double precision mode. This is unnecessary in order to meet any error requirement. However, the double precision mode is necessary in order to read information via the data declaration. The comment "EXTENSION" found in the margin of these subprograms refers to the fact that this particular type of data statement may not be available at other computer facilities.

```

//JOB AGUILAR,TIME=120
C
C DETERMINATION OF REATTACHMENT DISTANCE VS. REYNOLDS NUMBER
C USING THE BICKLEY EXACT SOLUTION FOR THE LAMINAR PLANE JET
C
      REAL K2
      DIMENSION ALPHA(5)
      READ(5,100)(ALPHA(I),I=1,5)
100  FORMAT(8F10.0)
      WRITE(6,200)
200  FORMAT(1H1,////19X,33HANALYSIS WITH THE BICKLEY PROFILE)
      PI=3.1415927
      PHIM=1.0471976
      DO 1 I=1,5
      XSI=PI*ALPHA(I)/(2.0*PHIM)
      BETAR=ATAN(2.0*PHIM*TAN(XSI)/PI)
      T=HTAN(BETAR)
C          WHERE T = HYPERBOLIC TANGENT FOUND IN EQN. 20
      S1=1.0/(36.0*T**3)-5.0/64.0
C          WHERE S1 = S/(B*RE) - EQN. 21
      K2=1.0-(2.0*PHIM/PI)**2
C          WHERE K2 = FACTOR OF SINE TERM IN EQN. 8
      S2=ELINT(K2,XSI)
C          WHERE S2 = S/A - EQN. 8
      C1=S1*SIN(XSI)/S2
      ALPHA(I)=180.0*ALPHA(I)/PI
      WRITE(6,300)ALPHA(I),C1
300  FORMAT(//23X,6HALPHA=,F5.2,5X,3HC1=,F7.4)
      1 CONTINUE
      STOP
      END

```

```
REAL FUNCTION HTAN(GAMMA)
C
C SOLUTION OF EQUATION 20 (MOMENTUM PRINCIPLE) VIA NEWTONS METHOD
C
  DIMENSION X(500)
  A=COS(GAMMA)
  X(1)=0.5
  DO 1 I=1,500
  X(I+1)=X(I)-((X(I)**3)-3.0*X(I)+2.0*A)/(3.0*(X(I)**2)-3.0)
  IF(ABS(X(I)-X(I+1)).LT.1.E-05)GO TO 2
1 CONTINUE
2 HTAN=X(I+1)
  RETURN
  END
```

```
REAL FUNCTION ELINT(Q,PHI)
```

```
C
C EVALUATION OF AN ELLIPTIC INTEGRAL OF THE SECOND KIND BY GAUSSIAN
C QUADRATURE USING 16 ORDINATES
C
```

```
REAL K
```

```
DOUBLE PRECISION XSI,W
```

```
DIMENSION XSI(16),W(16)
```

```
DATA(XSI(I),I=1,16)/-9.894009350D-01,-9.445750231D-01,-8.656312024
1D-01,-7.554044084D-01,-6.178762444D-01,-4.580167777D-01,-2.8160355
208D-01,-9.501250984D-02,9.501250984D-02,2.816035508D-01,4.58016777
37D-01,6.178762444D-01,7.554044084D-01,8.656312024D-01,9.445750231D
4-01,9.894009350D-01/
```

```
WHERE THE XSI(I) = ABSCISSAS
```

```
DA-5
```

```
DA-4
```

```
DATA(W(I),I=1,16)/2.715245941D-02,6.225352394D-02,9.515851168D-02,
11.246289713D-01,1.495959888D-01,1.691565194D-01,1.826034150D-01,1.
2894506105D-01,1.894506105D-01,1.826034150D-01,1.691565194D-01,1.49
35959888D-01,1.246289713D-01,9.51585117D-02,6.225352394D-02,2.71524
45941D-02/
```

```
WHERE THE W(I) = WEIGHTS
```

```
DA-5
```

```
DA-4
```

```
K=Q
```

```
XMAX=SIN(PHI)
```

```
WHERE X AND PHI = DUMMY VARIABLES OF INTEGRATION, AND XMAX
IS THE UPPER LIMIT
```

```
SUM=0.0
```

```
DO I M=1,16
```

```
X=XMAX*(XSI(M)+1.0)/2.0
```

```
Y=SQRT(1.0-K*X**2)/SQRT(1.0-X**2)
```

```
SUM=SUM+Y*W(M)
```

```
1 CONTINUE
```

```
ELINT=XMAX*SUM/2.0
```

```
RETURN
```

```
END
```

```
//GO.SYSIN
```

ANALYSIS WITH THE BICKLEY PROFILE

ALPHA=20.00 C1=-0.0194

ALPHA=25.00 C1=-0.0023

ALPHA=30.00 C1= 0.0248

ALPHA=40.00 C1= 0.1697

ALPHA=50.00 C1= 1.3624

OMPILE TIME= 3.25 SEC, EXECUTION TIME= 0.46 SEC, OBJECT CODE= 3296

```

//JOB AGUILAR,TIME=300
C
C DETERMINATION OF REATTACHMENT DISTANCE VS. REYNOLDS NUMBER USING
C THE OKABE APPROXIMATE SOLUTION FOR THE LAMINAR PLANE JET
C
      REAL LAMBDA,LAM,K2
      DIMENSION ALPHA(5)
      READ(5,100)(ALPHA(I),I=1,5)
100  FORMAT(8F10.0)
      WRITE(6,200)
200  FORMAT(1H1,////20X,31HANALYSIS WITH THE OKABE PROFILE)
      PI=3.1415927
      PHIM=1.0471976
      DO 1 I=1,5
      LAMBDA=LAM(ALPHA(I))
      S1=S(LAMBDA)
C          WHERE S1 = S/(B*RE) - EQN. 13
      XSI=PI*ALPHA(I)/(2.0*PHIM)
      K2=1.0-(2.0*PHIM/PI)**2
C          WHERE K2 = FACTOR OF SINE TERM IN EQN. 8
      S2=ELINT(K2,XSI)
C          WHERE S2 = S/A - EQN. 8
      C1=S1*SIN(XSI)/S2
      ALPHA(I)=180.0*ALPHA(I)/PI
      WRITE(6,300)ALPHA(I),C1
300  FORMAT(//23X,6HALPHA=,F5.2,5X,3HC1=,F7.4)
      1 CONTINUE
      STOP
      END

```

REAL FUNCTION LAM(Q)

C
C CALCULATION OF THE PARAMETER LAMBDA CORRESPONDING TO A GIVEN
C PLATE ANGLE ALPHA
C

REAL LM,MUM
DIMENSION LM(500)
PI=3.1415927
PHIR=0
PHIM=1.0471976
BETAR=ATAN(2.0*PHIM*TAN(PI*PHIR/(2.0*PHIM)))/PI
X=COS(BETAR)
LM(1)=1.20

C WHERE LM = LAMBDA

M=0

L=1

1 CONTINUE

M=M+1

ETAR=ORD(LM(M))

Y=D(LM(M))*MOM(LM(M),0.,ETAR)

C WHERE Y = COS(GAMMA) - EQN. 22

IF(ABS(X-Y).LT.1.E-06)GO TO 3

IF(X.LT.Y)GO TO 2

LM(M+1)=LM(M)-10.0**(-L)

GO TO 1

2 LM(1)=LM(M-1)

L=L+1

IF(L.GT.6)GO TO 3

M=0

GO TO 1

3 LAM=LM(M)

RETURN

END

```
REAL FUNCTION D(Q)
C
C CALCULATION OF THE DIMENSIONLESS JET WIDTH DELTA
C
REAL LM, MOM
LM=Q
C      WHERE LM = LAMBDA
IF(LM.LT.0.035)GO TO 1
D=1.0/MOM(LM,0.,1.)
RETURN
1 D=1.0+9.3788*LM/3.5
RETURN
END
```

```

REAL FUNCTION MOM(Q,S,T)
C
C INTEGRATION OF THETA0**2 OVER THE INTERVAL ETA = (S,T) AT LAMBDA
C
  REAL LM
  COMMON LM
  DIMENSION BINT(3),SINT(4)
  LM=Q
C
  WHERE LM = LAMBDA
  E=EXP(-1.0/LM)
  BINT(1)=VP(0,S,T)-6.0*V(0,1.,S,T)+15.0*V(0,2.,S,T)-20.0*V(0,3.,S,T
1)+15.0*V(0,4.,S,T)-6.0*V(0,5.,S,T)+V(0,6.,S,T)
  DO 1 K=1,4
  SINT(K)=VP(K,S,T)-3.0*V(K,1.,S,T)+3.0*V(K,2.,S,T)-V(K,3.,S,T)
1 CONTINUE
  BINT(2)=SINT(1)-3.0*SINT(2)+3.0*SINT(3)-SINT(4)
  BINT(3)=VP(2,S,T)-6.0*VP(3,S,T)+15.0*VP(4,S,T)-20.0*VP(5,S,T)+15.0
1*VP(6,S,T)-6.0*VP(7,S,T)+VP(8,S,T)
C
  WHERE BINT(1), SINT(1) ARE DEFINED IN EQN. 1A
  MOM=BINT(1)+(6.0*E/LM)*((1.0-E)**2)*BINT(2)+((3.0*E/LM)**2)*((1.0-
1E)**4)*BINT(3)
  RETURN
  END

```

```

REAL FUNCTION ORD(Q)
C
C CALCULATION OF THE ORDINATE OF THE REATTACHING STREAMLINE ETAR
C
REAL LM,INT
COMMON LM
DIMENSION INT(2),ETA(500)
ETA(1)=0.5
LM=Q
C      WHERE LM = LAMBDA
E=EXP(-1.0/LM)
DEL=D(LM)
C      WHERE DEL = DELTA
DO 1 J=1,500
INT(1)=3.0*V(0,1.,0.,ETA(J))-3.0*V(0,2.,0.,ETA(J))+V(0,3.,0.,ETA(J)
1))
INT(2)=VP(1,0.,ETA(J))-3.0*VP(2,0.,ETA(J))+3.0*VP(3,0.,ETA(J))-VP(
14,0.,ETA(J))
ETA(J+1)=INT(1)-((3.0*E/LM)*(1.0-E)**2)*INT(2)+1.0/DEL
IF(ABS(ETA(J+1)-ETA(J)).LT.1.E-06)GO TO 2
1 CONTINUE
2 ORD=ETA(J+1)
RETURN
END

```

REAL FUNCTION ELINT(Q,PHI)

```

C
C EVALUATION OF AN ELLIPTIC INTEGRAL OF THE SECOND KIND BY GAUSSIAN
C QUADRATURE USING 16 ORDINATES
C
  REAL K
  DOUBLE PRECISION XSI,W
  DIMENSION XSI(16),W(16)
  DATA(XSI(1),I=1,16)/-9.894009350D-01,-9.445750231D-01,-8.656312024
1D-01,-7.584044084D-01,-6.178762444D-01,-4.580167777D-01,-2.8160355
298D-01,-9.501250984D-02,9.501250984D-02,2.816035508D-01,4.58016777
37D-01,6.178762444D-01,7.554044084D-01,8.656312024D-01,9.445750231D
4-01,9.894009350D-01/
C      WHERE THE XSI(I) = ABSCISSAS
ION*      DA-5
ION*      DA-4
  DATA(W(I),I=1,16)/2.715245941D-02,6.225352394D-02,9.515851168D-02,
11.246289713D-01,1.495959888D-01,1.691565194D-01,1.826034150D-01,1.
2894506105D-01,1.894506105D-01,1.826034150D-01,1.691565194D-01,1.49
35959888D-01,1.246289713D-01,9.51585117D-02,6.225352394D-02,2.71524
45941D-02/
C      WHERE THE W(I) = WEIGHTS
ION*      DA-5
ION*      DA-4
  K=Q
  XMAX=SIN(PHI)
C      WHERE X AND PHI = DUMMY VARIABLES OF INTEGRATION, AND XMAX
C      IS THE UPPER LIMIT
  SUM=0.0
  DO 1 M=1,16
  X=XMAX*(XSI(M)+1.0)/2.0
  Y=SQRT(1.0-K*X**2)/SQRT(1.0-X**2)
  SUM=SUM+Y*W(M)
1 CONTINUE
  ELINT=XMAX*SUM/2.0
  RETURN
  END

```

REAL FUNCTION S(Q)

```

C
C CALCULATION OF S/(8*RE) FROM EQUATION 13 BY GAUSSIAN QUADRATURE
C USING 16 ORDINATES
C
  REAL LM,LMMAX
  DOUBLE PRECISION XSI,W
  DIMENSION XSI(16),W(16)
  DATA(XSI(I),I=1,16)/-9.894009350D-01,-9.445750231D-01,-8.656312024
1D-01,-7.554044084D-01,-6.178762444D-01,-4.580167777D-01,-2.8160355
208D-01,-9.501250984D-02,9.501250984D-02,2.816035508D-01,4.58016777
37D-01,6.178762444D-01,7.554044084D-01,8.656312024D-01,9.445750231D
4-01,9.894009350D-01/
C
  WHERE THE XSI(I) = ABSCISSAS
ION*   DA-5
ION*   DA-4
  DATA(W(I),I=1,16)/2.715245941D-02,6.225352394D-02,9.515851168D-02,
11.246289713D-01,1.495959888D-01,1.691565194D-01,1.826034150D-01,1.
2894506105D-01,1.894506105D-01,1.826034150D-01,1.691565194D-01,1.49
35959888D-01,1.246289713D-01,9.51585117D-02,6.225352394D-02,2.71524
45941D-02/
C
  WHERE THE W(I) = WEIGHTS
ION*   DA-5
ION*   DA-4
  LMMAX=Q
C
  WHERE LM = LAMBDA, AND LMMAX IS THE UPPER LIMIT
  SUM=0.0
  DO 1 J=1,16
  LM=LMMAX*(XSI(J)+1.0)/2.0
  E=EXP(-1.0/LM)
  Y=((D(LM)**2)*(1.0-E)**4)/((1.0-3.0*E)+6.0*LM*(1.0-E))
  SUM=SUM+Y*W(J)
1 CONTINUE
  S=LMMAX*SUM/8.0
  RETURN
  END

```

```

REAL FUNCTION V(N,XN,C,D)
C
C INTEGRATION OF (E*X)**N*EXP(A*X) OVER THE INTERVAL (C,D)
C
COMMON Z
DIMENSION XINT(2)
A=XN/Z
DO 6 L=1,2
IF(L.EQ.1)X=D
IF(L.EQ.2)X=C
FACTN=1.0
C      WHERE FACTN = N FACTORIAL
IF(N.EQ.0)GO TO 2
DO 1 I=1,N
B=1
FACTN=FACTN*B
1 CONTINUE
2 SUM=0.0
M=N+1
DO 5 K=1,M
FACTNK=1.0
C      WHERE FACTNK = (N-K+1) FACTORIAL
IF(K.EQ.M)GO TO 4
J=N-K+1
DO 3 I=1,J
B=I
FACTNK=FACTNK*B
3 CONTINUE
S=((-1.0)**(K-1))*(FACTN*X**(N-K+1))/(FACTNK*A**K)
4 IF(K.EQ.M)S=((-1.0)**(K-1))*(FACTN/A**K)
SUM=SUM+S
5 CONTINUE
XINT(L)=SUM*EXP(A*(X-1.0))
6 CONTINUE
V=XINT(1)-XINT(2)
RETURN
END

```

```
      REAL FUNCTION VP(N,A,B)
C
C  INTEGRATION OF X**N OVER THE INTERVAL (A,B)
C
      XN=N
      VP=(B**(N+1)-A**(N+1))/(XN+1.0)
      RETURN
      END

//GO.SYSIN
```

ANALYSIS WITH THE OKABE PROFILE

ALPHA=20.00 C1= 0.0398

ALPHA=25.00 C1= 0.0619

ALPHA=30.00 C1= 0.0954

ALPHA=40.00 C1= 0.2561

ALPHA=50.00 C1= 1.4416

COMPILE TIME= 9.09 SEC, EXECUTION TIME= 243.41 SEC, OBJECT CODE= 1016

```

//JOB AGUILAR,TIME=1000
C
C DETERMINATION OF REATTACHMENT DISTANCE VS. REYNOLDS NUMBER USING
C THE MODIFIED OKABE APPROXIMATE SOLUTION FOR THE LAMINAR PLANE JET
C
      REAL LAMBDA,LAM,K2
      DIMENSION ALPHA(5)
      READ(5,100)(ALPHA(I),I=1,5)
100  FORMAT(8F10.0)
      WRITE(6,200)
200  FORMAT(1H1,////16X,40HANALYSIS WITH THE MODIFIED OKABE PROFILE)
      PI=3.1415927
      PHIM=1.0471976
      DO 1 I=1,5
      LAMBDA=LAM(ALPHA(I))
      S1=S(LAMBDA)
C      WHERE S1 = S/(B*RE) - EQN. 18
      XSI=PI*ALPHA(I)/(2.0*PHIM)
      K2=1.0-(2.0*PHIM/PI)**2
C      WHERE K2 = FACTOR OF SINE TERM IN EQN. 8
      S2=ELINT(K2,XSI)
C      WHERE S2 = S/A - EQN. 8
      C1=S1*SIN(XSI)/S2
      ALPHA(I)=180.0*ALPHA(I)/PI
      WRITE(6,300)ALPHA(I),C1
300  FORMAT(//23X,6HALPHA=,F5.2,5X,3HC1=,F7.4)
      1 CONTINUE
      STOP
      END

```

REAL FUNCTION LAM(Q)

C
C CALCULATION OF THE PARAMETER LAMBDA CORRESPONDING TO A GIVEN
C PLATE ANGLE ALPHA
C

REAL LM,MOM
DIMENSION LM(500)
PI=3.1415927
PHIR=Q
PHIM=1.0471976
BETAR=ATAN(2.0*PHIM*TAN(PI*PHIR/(2.0*PHIM)))/PI
X=COS(BETAR)
LM(1)=0.95

C WHERE LM = LAMBDA

M=0

L=1

1 CONTINUE

M=M+1

ETAR=ORD(LM(M))

Y=5.0*D(LM(M))*MOM(LM(M),0.,ETAR)/6.0

C WHERE Y = COS(GAMMA) - EQN. 24

IF(ABS(X-Y).LT.1.E-06)GO TO 3

IF(X.LT.Y)GO TO 2

LM(M+1)=LM(M)-10.0**(-L)

GO TO 1

2 LM(1)=LM(M-1)

L=L+1

IF(L.GT.6)GO TO 3

M=0

GO TO 1

3 LAM=LM(M)

RETURN

END

REAL FUNCTION D(Q)

```
C
C CALCULATION OF THE DIMENSIONLESS JET WIDTH DELTA
C
  REAL LM, MOM
  LM=Q
C      WHERE LM = LAMBDA
  IF(LM.LT.0.038)GO TO 1
  D=6.0/(5.0*MOM(LM,0.,1.))
  RETURN
1 D=1.0+3.385*LM/38.0
  RETURN
  END
```

```

REAL FUNCTION MUM(Q,S,T)
C
C INTEGRATION OF THETAM**2 OVER THE INTERVAL ETA = (S,T) AT LAMBDA
C
REAL LM
COMMON LM
DIMENSION BINT(3),SINT(9)
LM=Q
C      WHERE LM = LAMBDA
E=EXP(-1.0/LM)
DO 1 L=2,6,2
K=L-2
M=L/2
SINT(M)=VP(K,S,T)-6.0*V(K,1.,S,T)+15.0*V(K,2.,S,T)-20.0*V(K,3.,S,T
1)+15.0*V(K,4.,S,T)-6.0*V(K,5.,S,T)+V(K,6.,S,T)
1 CONTINUE
BINT(1)=SINT(1)-2.0*SINT(2)+SINT(3)
DO 2 L=4,9
K=L-3
SINT(L)=VP(K,S,T)-3.0*V(K,1.,S,T)+3.0*V(K,2.,S,T)-V(K,3.,S,T)
2 CONTINUE
BINT(2)=SINT(4)-3.0*SINT(5)+2.0*SINT(6)+2.0*SINT(7)-3.0*SINT(8)+SI
INT(9)
BINT(3)=VP(2,S,T)-6.0*VP(3,S,T)+15.0*VP(4,S,T)-20.0*VP(5,S,T)+15.0
1*VP(6,S,T)-6.0*VP(7,S,T)+VP(8,S,T)
C      WHERE BINT(I), SINT(I) ARE DEFINED IN EQN. 2A
VALUE=BINT(1)+6.0*(E/LM)*((1.0-E)**2)*BINT(2)+(9.0*((E/LM)*(1.0-E)
1**2)**2)*BINT(3)
MUM=9.0*VALUE/4.0
RETURN
END

```

```
REAL FUNCTION ORD(Q)
```

```
C
C CALCULATION OF THE ORDINATE OF THE REATTACHING STREAMLINE ETAR
C
```

```
REAL LM,INT
COMMON LM
DIMENSION INT(3),ETA(1000)
LM=Q
```

```
C WHERE LM = LAMBDA
C DEL=D(LM)
C WHERE DEL = DELTA
```

```
ETA(1)=0.5
E=EXP(-1.0/LM)
DO 1 J=1,1000
INT(1)=3.0*V(0,1.,0.,ETA(J))-3.0*V(0,2.,0.,ETA(J))+V(0,3.,0.,ETA(J)
1)
INT(2)=VP(2,0.,ETA(J))-3.0*V(2,1.,0.,ETA(J))+3.0*V(2,2.,0.,ETA(J))
1-V(2,3.,0.,ETA(J))
INT(3)=-VP(1,0.0,ETA(J))+3.0*VP(2,0.0,ETA(J))-3.0*VP(3,0.0,ETA(J))
1+VP(4,0.0,ETA(J))
ETA(J+1)=INT(1)+INT(2)+((3.0*E/LM)*(1.0-E)**2)*INT(3)+2.0/(3.0*DEL
1)
```

```
IF(ABS(ETA(J+1)-ETA(J)).LT.1.E-06)GO TO 2
```

```
1 CONTINUE
2 ORD=ETA(J+1)
RETURN
END
```

REAL FUNCTION ELINT(Q,PHI)

```

C
C EVALUATION OF AN ELLIPTIC INTEGRAL OF THE SECOND KIND BY GAUSSIAN
C QUADRATURE USING 16 ORDINATES
C
  REAL K
  DOUBLE PRECISION XSI,W
  DIMENSION XSI(16),W(16)
  DATA(XSI(I),I=1,16)/-9.894009350D-01,-9.445750231D-01,-8.656312024
1D-01,-7.554044084D-01,-6.178762444D-01,-4.580167777D-01,-2.8160355
208D-01,-9.501250984D-02,9.501250984D-02,2.816035508D-01,4.58016777
37D-01,6.178762444D-01,7.554044084D-01,8.656312024D-01,9.445750231D
4-01,9.894009350D-01/
      WHERE THE XSI(I) = ABSCISSAS
      DA-5
      DA-4
  DATA(W(I),I=1,16)/2.715245941D-02,6.225352394D-02,9.515851168D-02,
11.246289713D-01,1.495959888D-01,1.691565194D-01,1.826034150D-01,1.
2894506105D-01,1.894506105D-01,1.826034150D-01,1.691565194D-01,1.49
35959888D-01,1.246289713D-01,9.51585117D-02,6.225352394D-02,2.71524
45941D-02/
      WHERE THE W(I) = WEIGHTS
      DA-5
      DA-4
  K=Q
  XMAX=SIN(PHI)
      WHERE X AND PHI = DUMMY VARIABLES OF INTEGRATION, AND XMAX
      IS THE UPPER LIMIT
  SUM=0.0
  DO 1 M=1,16
  X=XMAX*(XSI(M)+1.0)/2.0
  Y=SQRT(1.0-K*X**2)/SQRT(1.0-X**2)
  SUM=SUM+Y*W(M)
1 CONTINUE
  ELINT=XMAX*SUM/2.0
  RETURN
  END

```

REAL FUNCTION S(Q)

C
C CALCULATION OF S/(B*RE) FROM EQUATION 18 BY GAUSSIAN QUADRATURE
C WITH 16 ORDINATES
C

REAL LM,LMMAX
DOUBLE PRECISION XSI,W
DIMENSION XSI(16),W(16)
DATA(XSI(I),I=1,16)/-9.894009350D-01,-9.445750231D-01,-8.656312024
1D-01,-7.554044084D-01,-6.178762444D-01,-4.580167777D-01,-2.8160355
208D-01,-9.501250984D-02,9.501250984D-02,2.816035508D-01,4.58016777
37D-01,6.178762444D-01,7.554044084D-01,8.656312024D-01,9.445750231D
4-01,9.894009350D-01/

WHERE THE XSI(I) = ABSCISSAS

DA-5

DA-4

DATA(W(I),I=1,16)/2.715245941D-02,6.225352394D-02,9.515851168D-02,
11.246289713D-01,1.495959888D-01,1.691565194D-01,1.826034150D-01,1.
2894506105D-01,1.894506105D-01,1.826034150D-01,1.691565194D-01,1.49
35959888D-01,1.246289713D-01,9.51585117D-02,6.225352394D-02,2.71524
45941D-02/

WHERE THE W(I) = WEIGHTS

DA-5

DA-4

LMMAX=Q

WHERE LM = LAMBDA, AND LMMAX IS THE UPPER LIMIT

SUM=0.0

DO 1 J=1,16

LM=LMMAX*(XSI(J)+1.0)/2.0

E=EXP(-1.0/LM)

Y=((D(LM)**2)*E*(1.0-E)**4)/(3.0*E*((1.0-3.0*E)+6.0*LM*(1.0-E))+2.
10*(LM*(1.0-E))**2)

SUM=SUM+Y*W(J)

1 CONTINUE

S=9.0*LMMAX*SUM/16.0

RETURN

END

```

REAL FUNCTION V(N,XN,C,D)
C
C INTEGRATION OF (E*X)**N*EXP(A*X) OVER THE INTERVAL (C,D)
C
COMMON Z
DIMENSION XINT(2)
A=XN/Z
DO 6 L=1,2
IF(L.EQ.1)X=D
IF(L.EQ.2)X=C
FACTN=1.0
C      WHERE FACTN = N FACTORIAL
IF(N.EQ.0)GO TO 2
DO 1 I=1,N
B=I
FACTN=FACTN*B
1 CONTINUE
2 SUM=0.0
M=N+1
DO 5 K=1,M
FACTNK=1.0
C      WHERE FACTNK = (N-K+1) FACTORIAL
IF(K.EQ.M)GO TO 4
J=N-K+1
DO 3 I=1,J
B=I
FACTNK=FACTNK*B
3 CONTINUE
S=((-1.0)**(K-1))*(FACTN*X**(N-K+1))/(FACTNK*A**K)
4 IF(K.EQ.M)S=((-1.0)**(K-1))*(FACTN/A**K)
SUM=SUM+S
5 CONTINUE
XINT(L)=SUM*EXP(A*(X-1.0))
6 CONTINUE
V=XINT(1)-XINT(2)
RETURN
END

```

```
      REAL FUNCTION VP(N,A,B)
C
C  INTEGRATION OF X**N OVER THE INTERVAL (A,B)
C
      XN=N
      VP=(B**(N+1)-A**(N+1))/(XN+1.0)
      RETURN
      END

//GD.SYSIN
```

ANALYSIS WITH THE MODIFIED OKABE PROFILE

ALPHA=20.00 CI= 0.0249

ALPHA=25.00 CI= 0.0401

ALPHA=30.00 CI= 0.0640

ALPHA=40.00 CI= 0.1869

ALPHA=50.00 CI= 1.2306

COMPILE TIME= 10.60 SEC, EXECUTION TIME= 819.79 SEC, OBJECT CODE= 10904

Appendix D

Comments on Thomas' Modification of the Okabe Solution

Thomas' proposal for the modification of the Okabe approximate solution for the plane laminar jet appears in equation 15. Along with including the effect of a fully developed velocity profile at the nozzle exit, Thomas' analysis includes the effect of pressure gradient on jet development as well. To this end, he postulates the following:

$$-\frac{1}{\rho} \frac{\partial P}{\partial x} = \frac{\tau_o}{\rho \Delta} \left(1 - e^{-\frac{\eta_o - \eta}{\eta_o \lambda}} \right)^3 \quad (1D)$$

where τ_o = the shear stress at the wall within the rectangular slot
from which the jet issues

$\eta_o = \eta$ at which $\frac{\partial P}{\partial x}$ goes to zero

Thomas continues by asserting that at the origin,

$$u = U \left(1 - \frac{y^2}{\Delta^2} \right)$$

and that

$$\tau_o = \frac{2\mu U}{\Delta} .$$

It can be seen from equation 1D that for all $\eta < \eta_o$ and for all $\lambda \geq 0$, the pressure gradient is negative.

It is the present author's assertion that equation 1D leads to conclusions which from intuition are unacceptable. The boundary layer equation in the x-direction is

$$u \frac{\partial u}{\partial x} + v \frac{\partial u}{\partial y} = - \frac{1}{\rho} \frac{\partial P}{\partial x} + v \frac{\partial^2 u}{\partial y^2}$$

and the equation of continuity is

$$\frac{\partial u}{\partial x} + \frac{\partial v}{\partial y} = 0 .$$

Integration over half the width of the jet results in

$$\int_0^{\Delta} u \frac{\partial u}{\partial x} dy + \int_0^{\Delta} v \frac{\partial u}{\partial y} dy = - \frac{1}{\rho} \int_0^{\Delta} \frac{\partial P}{\partial x} dy + v \int_0^{\Delta} \frac{\partial^2 u}{\partial y^2} dy . \quad (2D)$$

term 1 term 2 term 3 term 4

One should note that $\Delta = \Delta(x)$. Turning attention to term 1, it is seen that

$$\int_0^{\Delta} u \frac{\partial u}{\partial x} dy = \frac{1}{2} \int_0^{\Delta} \frac{\partial}{\partial x} (u^2) dy = \frac{1}{2} \frac{d}{dx} \int_0^{\Delta} u^2 dy - \frac{1}{2} u(x, \Delta)^2 \frac{d\Delta}{dx}$$

But $u(x, \Delta) = 0$,

$$\int_0^{\Delta} u \frac{\partial u}{\partial x} dy = \frac{1}{2} \frac{d}{dx} \int_0^{\Delta} u^2 dy. \quad (3D)$$

From the equation of continuity,

$$v = - \int_0^y \frac{\partial u}{\partial x} dy$$

Substituting into term 2 of equation 2D,

$$\int_0^{\Delta} v \frac{\partial u}{\partial y} dy = - \int_0^{\Delta} \frac{\partial u}{\partial y} \int_0^y \frac{\partial u}{\partial x} dy dy$$

Integration by parts gives

$$\int_0^{\Delta} v \frac{\partial u}{\partial y} dy = - \left[u \int_0^y \frac{\partial u}{\partial x} dy \right]_0^{\Delta} + \int_0^{\Delta} u \frac{\partial u}{\partial x} dy$$

But $u(x, \Delta) = 0$ and $\int_0^0 \frac{\partial u}{\partial x} dy = 0$,

$$\int_0^{\Delta} v \frac{\partial u}{\partial y} dy = \int_0^{\Delta} u \frac{\partial u}{\partial x} dy,$$

and from equation 3D,

$$\int_0^{\Delta} v \frac{\partial u}{\partial y} dy = \frac{1}{2} \frac{d}{dx} \int_0^{\Delta} u^2 dy . \quad (4D)$$

Considering term 4 of equation 2D,

$$v \int_0^{\Delta} \frac{\partial^2 u}{\partial y^2} dy = v \left[\frac{\partial u}{\partial y} \right]_0^{\Delta} = 0 . \quad (5D)$$

Substitution for terms 1, 2, and 4 of equation 2D yields

$$\frac{d}{dx} \int_0^{\Delta} \rho u^2 dy = - \int_0^{\Delta} \frac{\partial P}{\partial x} dy .$$

But the momentum $J = 2 \int_0^{\Delta} \rho u^2 dy$ and therefore

$$\frac{dJ}{dx} = -2 \int_0^{\Delta} \frac{\partial P}{\partial x} dy .$$

Substitution for $\partial P/\partial x$ gives

$$\frac{dJ}{dx} = 2 \int_0^{\Delta} \frac{2\mu U}{\Delta^2} (1 - \epsilon e^{\eta/\eta_0 \lambda})^3 dy .$$

Since $\eta_0 \leq 1$ and since $\partial P/\partial x = 0$ for $\eta > \eta_0$,

$$\frac{dJ}{dx} = \frac{4\mu U}{\Delta} \int_0^{\eta_0} (1 - \epsilon e^{\eta/\eta_0 \lambda})^3 d\eta .$$

Integration yields,

$$\frac{dJ}{dx} = \frac{4\mu U \eta_0}{\Delta} \left[1 - 3(\lambda - \lambda \epsilon) + \frac{3}{2} (\lambda - \lambda \epsilon^2) - \frac{1}{3} (\lambda - \lambda \epsilon^3) \right] . \quad (6D)$$

It can be easily shown from equation 6D that dJ/dx is positive for all finite λ and that only as $\lambda \rightarrow \infty$ does $dJ/dx \rightarrow 0$. Therefore, momentum has been shown never to decrease with distance. Thomas' calculations* support these assertions: at $\lambda = 1.3$, jet momentum has increased by 20% of its value at $\lambda = 0$.

* Thomas, A. L., "Force and Mass Balances of the Incompressible, Isothermal, Planar Laminar Jet Issuing From a Finite Source," AD 115055, Tables 1 and 2.

The assertion that Thomas has overly valued the influence of the pressure gradient may be demonstrated in another manner. It has been shown previously that one may expect the cosine of the reattachment angle (equation 2) to approach zero strictly monotonically as reattachment distance is infinitely increased. If Thomas' velocity profile is used in the calculation of reattachment distance, it is seen that indeed,

$$\lim_{X_r \rightarrow \infty} \cos \gamma = 0,$$

but also that the $\cos \gamma$ approaches zero much too slowly. This, of course, results in completely unrealistic values of reattachment distance.

The author hopes that the reader does not detect an air of self-righteousness in the preceding comments. The author hardly can afford such an attitude, because his alternate proposal for the velocity profile is vulnerable to criticism as well. For instance, for values of the parameter $\lambda < 0.12$, the equation of continuity is not satisfied. However, since the investigation is concerned only with jet reattachment to an adjacent plate and since this corresponds to a range of λ of $0.2 \rightarrow 0.9$, the author feels justified in his use of the modified Okabe profile.

AN ANALYSIS OF LAMINAR JET REATTACHMENT:
REATTACHMENT DISTANCE AS A FUNCTION OF REYNOLDS NUMBER

by

Felix Aguilar

Abstract

The problem of laminar jet reattachment to an inclined flat plate was attacked by the application of the momentum equation at the reattachment point. The pressure distribution within the separation bubble was considered in the analysis as well as the initial state of development of the reattaching jet. The assumption was also made that reattachment angle was independent of Reynolds number for a given plate inclination. A general solution was developed in which reattachment distance was determined to be directly proportional to Reynolds number.

The theory correlated moderately well with experiment at a plate inclination of 30° , but it clearly failed at all other angles of inclination. It was shown that the initial state of jet development had a first order effect on the reattachment phenomenon.